# Interaction of high-intensity beam with structured solid surface plasma in relativistic regime

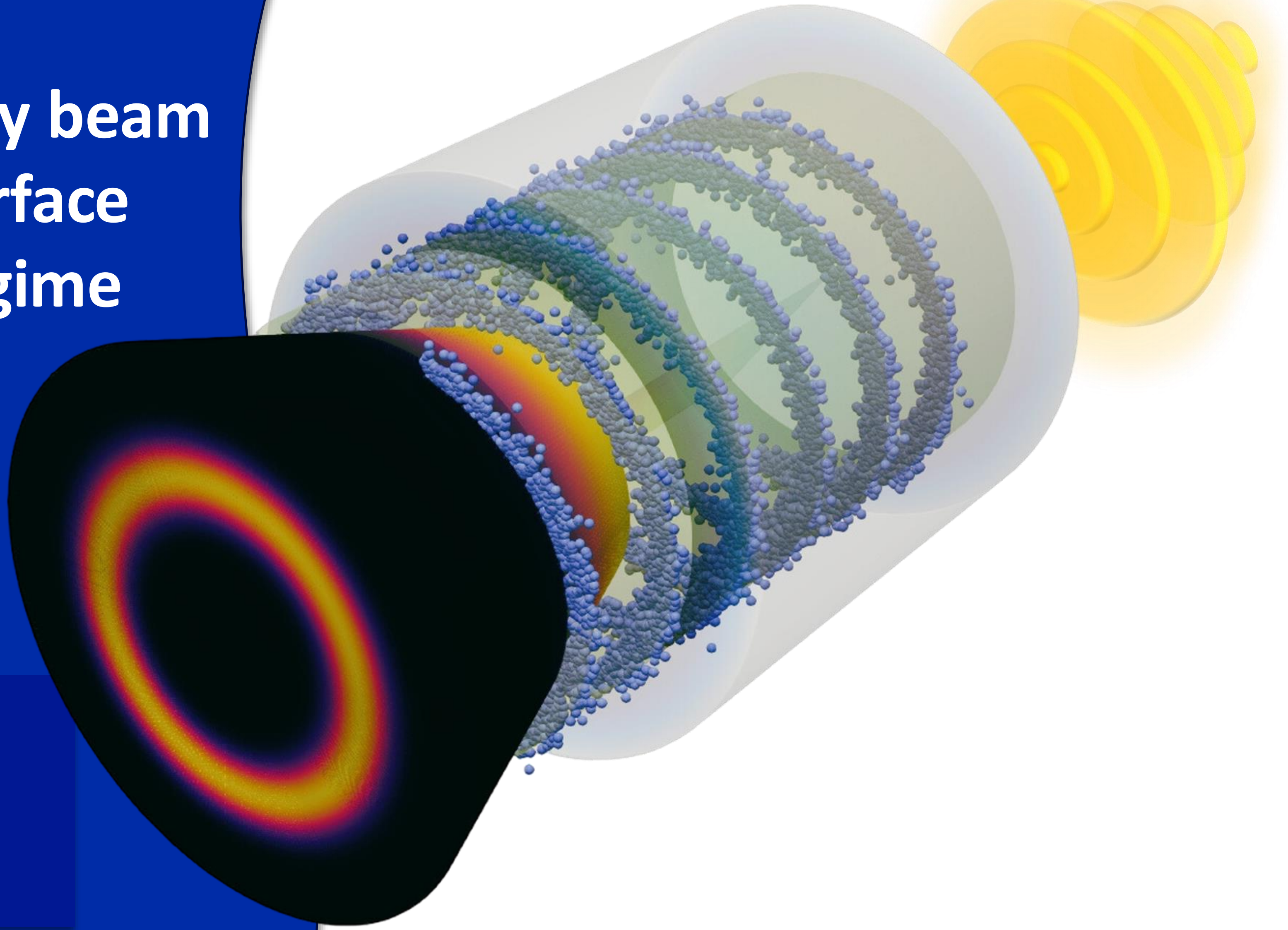

**3rd nanoAc2025 Workshop**

https://indico.ph.liv.ac.uk/e/nanoac2025

**Dr. Bifeng Lei**

bifeng.lei@liverpool.ac.uk

University of Liverpool / The Cockcroft Institute

6 November 2025

Novotel Paddington Village, Liverpool, UK

The Cockcroft Institute of Accelerator Science and Technology

UNIVERSITY OF LIVERPOOL

QUASAR GROUP

# Contents

**Motivations**

- Energy frontier
- Gate-free RSP
- Ultra-compact acc./radiation

**Theory of relativistic surface plasmon**

- Eigen RSP modes
- Dispersion relation
- Curvature effects
- Pre-plasma effects

**Surface plasma-based wakefield acceleration**

- Leaky wakefield on sharp surface
- Bubble wakefield on soft surface

**RSP-based Coherent radiation generation**

- RSP excitation inside microtube
- Mode selection
- CSR emission

**Experimental potentials**

- Potential facilities
- Experimental opportunities

# Big Motivation : Energy Frontier

## Towards TeV/m plasma-based acceleration

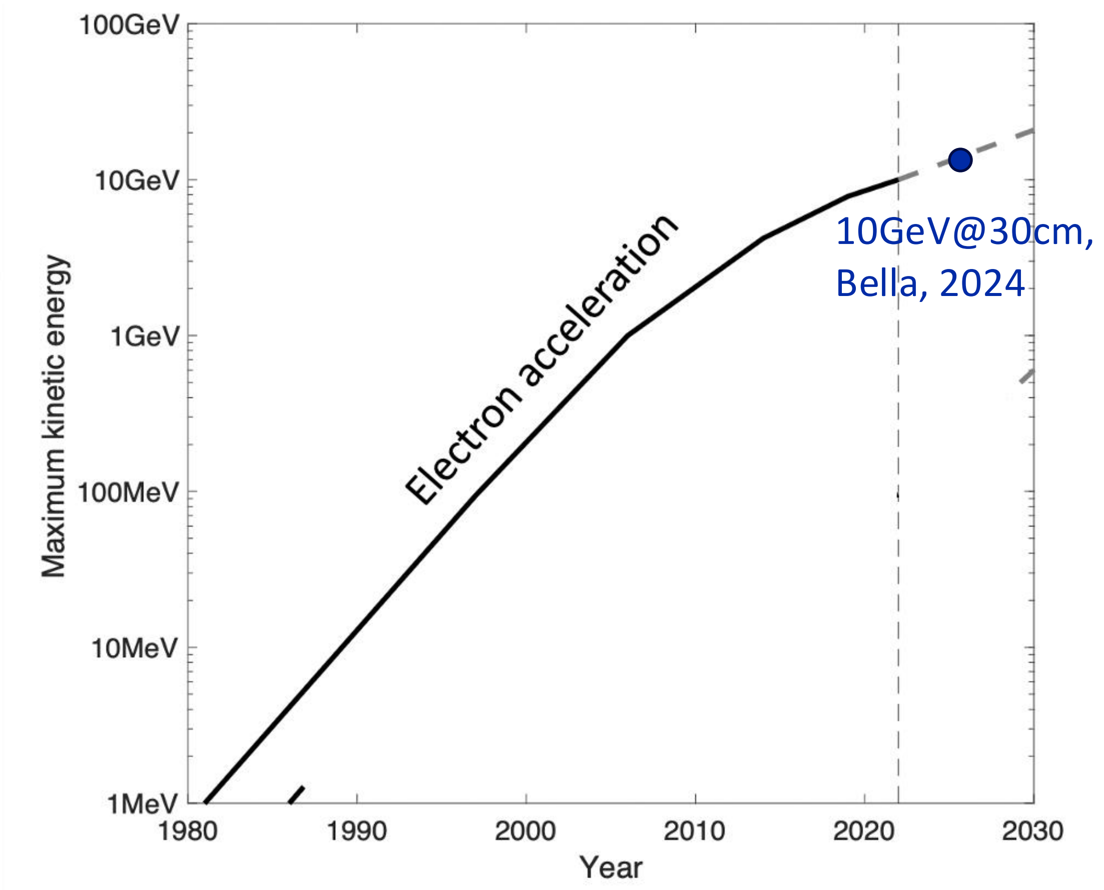


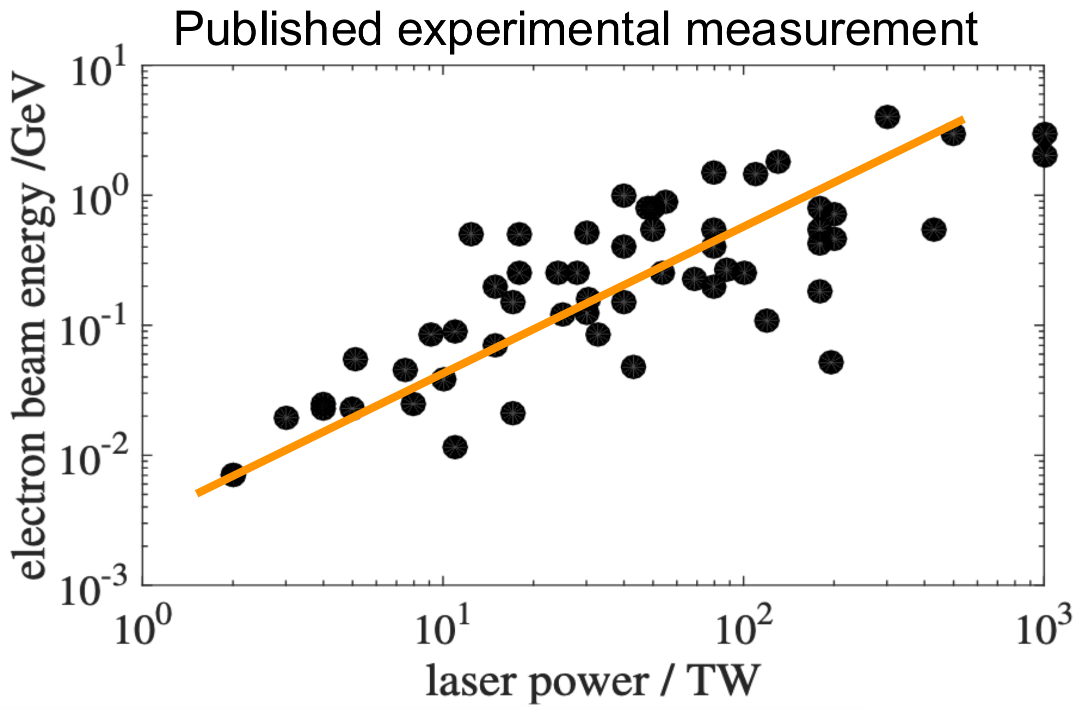


Scales with infinite laser power? -- > **NO,** due to strong instabilities!!

# Big Motivation : Energy Frontier

## Towards TeV/m plasma-based acceleration

New scale with solid surface plasma?

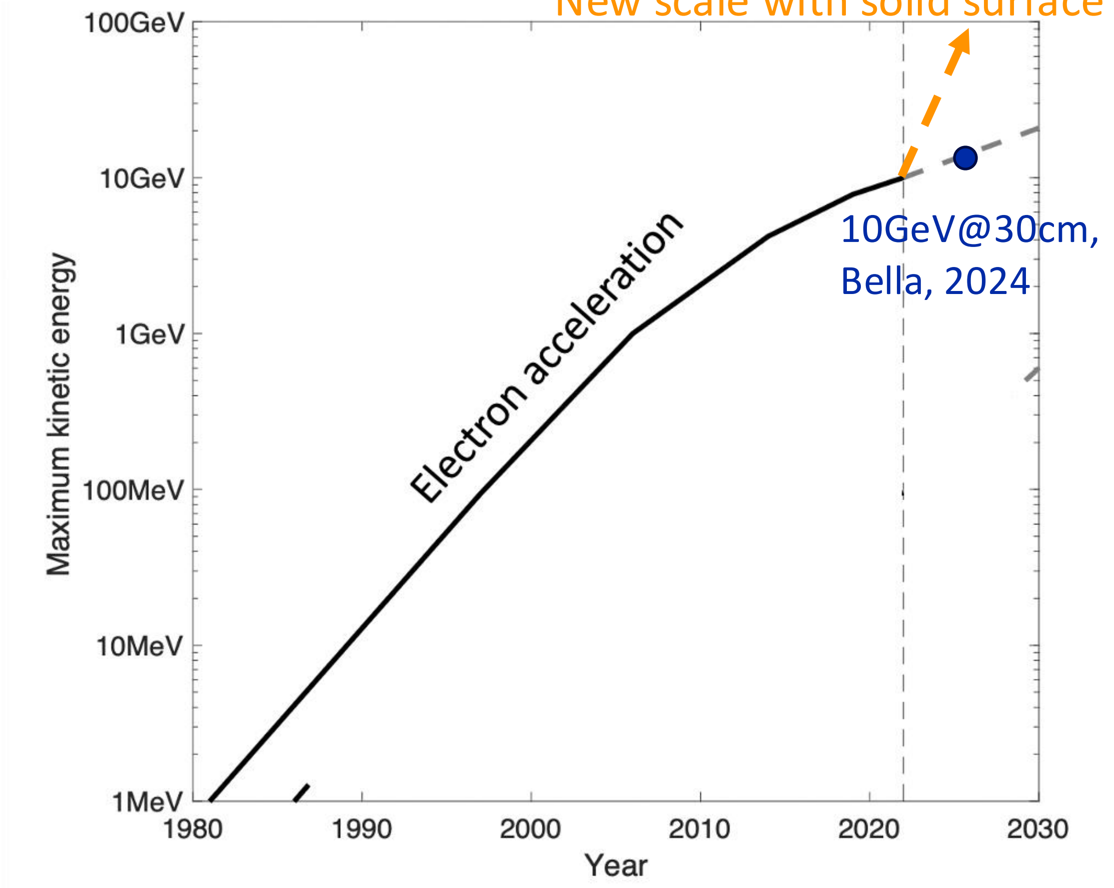


Scales with infinitely dense plasma?

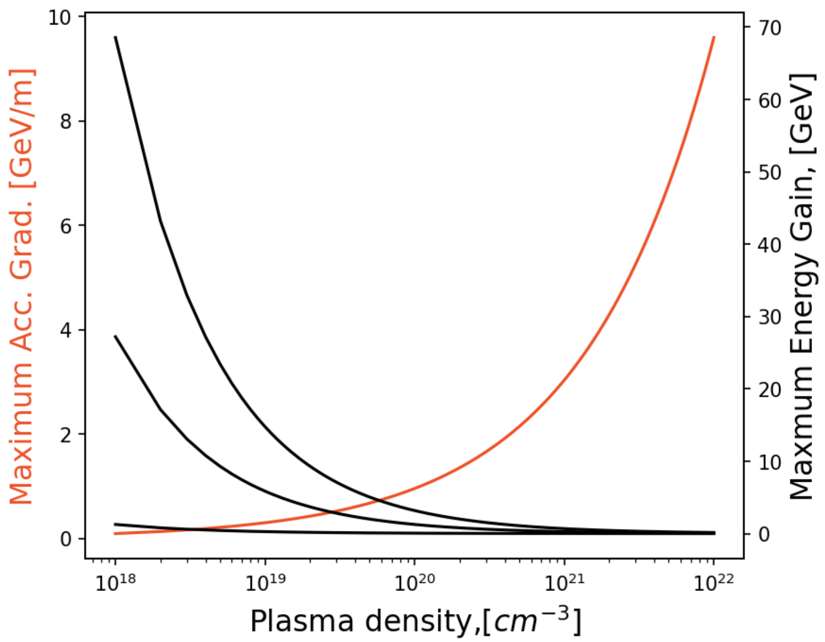


-- > **NO!!** Limited by laser penetration :

$$n_c = \frac{m_e c^2}{4\pi e^2 \lambda_0^2}$$

# Big Motivation : Energy Frontier

Towards TeV/m plasma-based acceleration

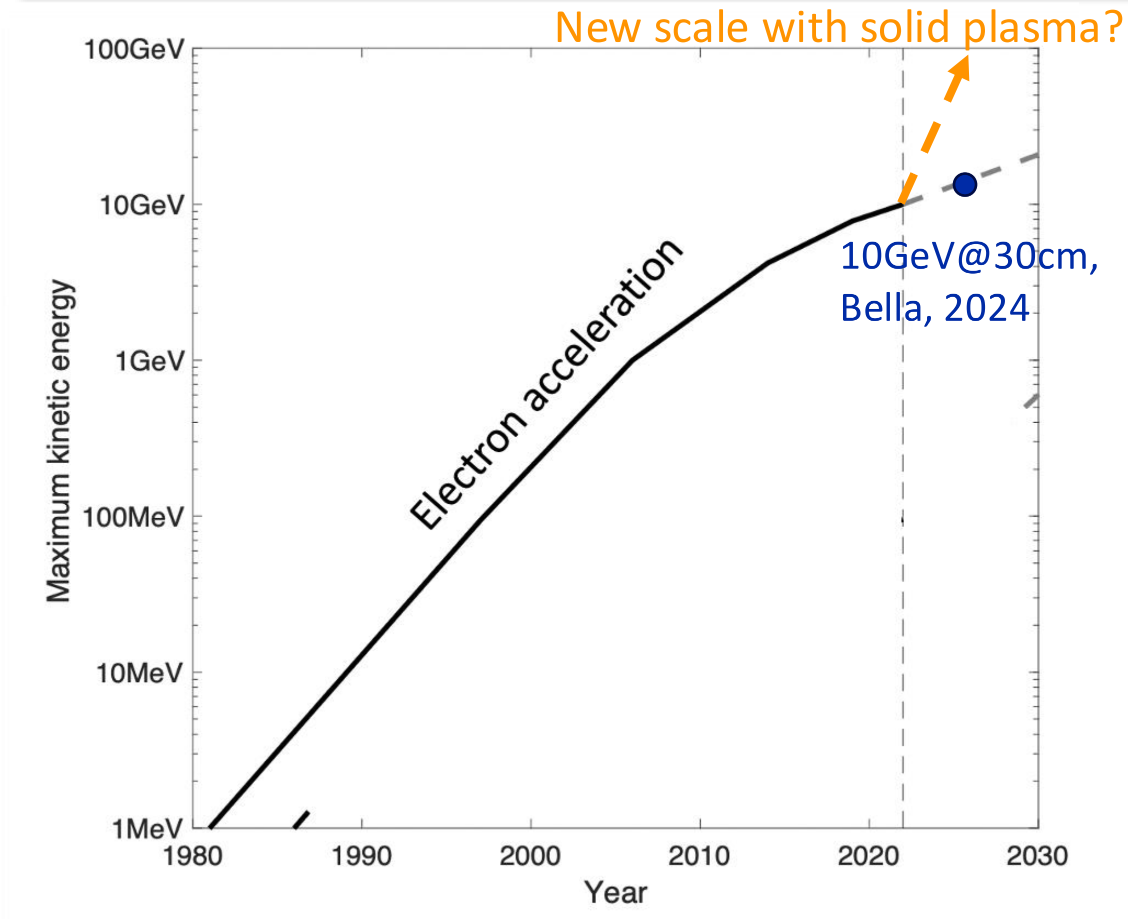


**Why solid surface plasma?**

- High density
- Ultrahigh field
- Stable Propagation
- Energy efficiency
- Flexible structures
- …

# Big Motivation : Gate-free

## New region of Surface Plasmon

Planar microtape

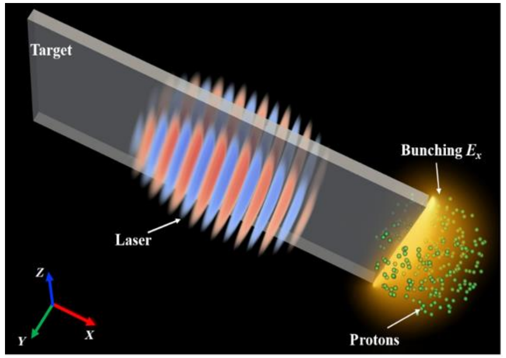


Shen et al. PRX 11, 041002 (2021)

Experiments (Flat)

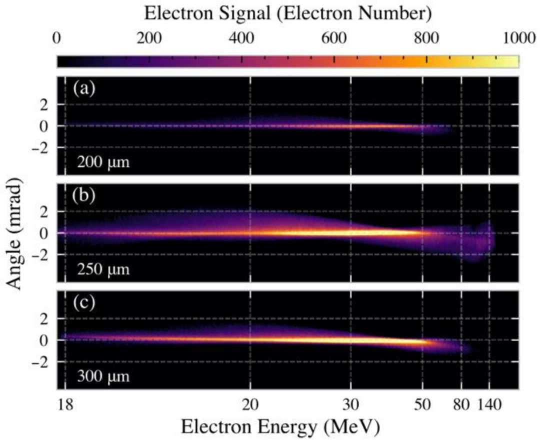


McCay et al. PRL. 135, 145001 (2025)

Cylindrical microtube

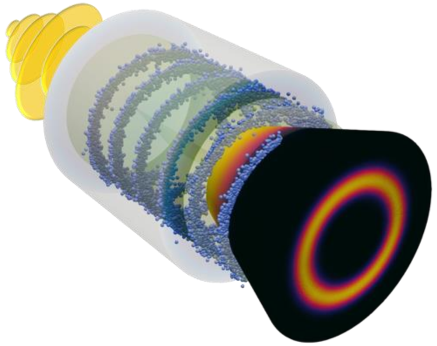

B. Lei et al. PRL. 135, 205001 (2025)

End-coupling SP excitation

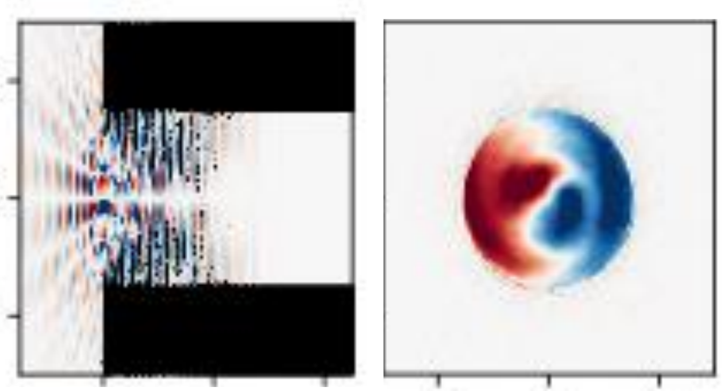

**A method suitable for high-intensity laser and particle beams in relativistic regime.**

# Big Motivation : Ultra-compact

## Ultra-high gradient acceleration & radiation

Gaseous Bulk Plasma
LWFA@HIJ

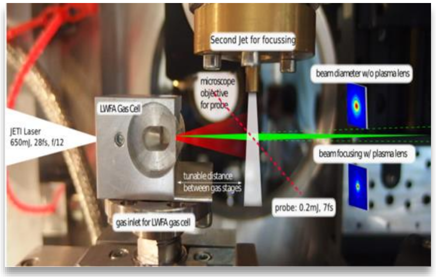


Solid surface plasma
CNT@UOL, UOM, UOV,…

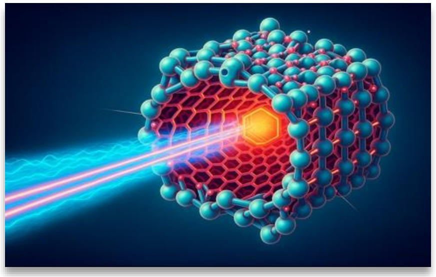

**m@MV/m**

**µm@TV/m**

**mm@GV/m**

**nm@PV/m**

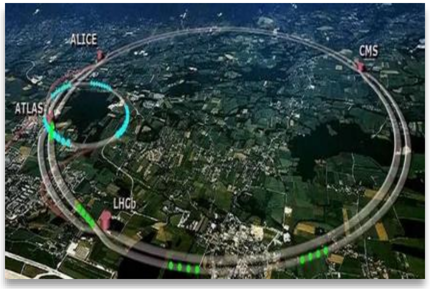


Metal Cavity
LHC@CERN

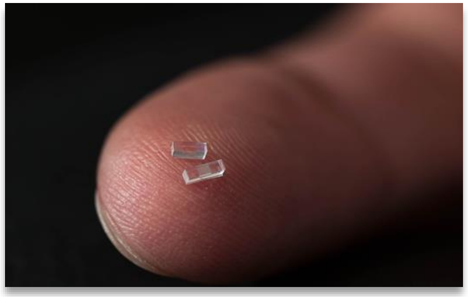

Solid dielectric
DLA@ SLAC&TUD

# Nonlinear Theory of Relativistic Surface Plasmons (RSPs) and Wakefields

- General theory of RSP fields
- Dispersion relation
- Surface geometric effects
- Soft surface and Pre-plasma effects

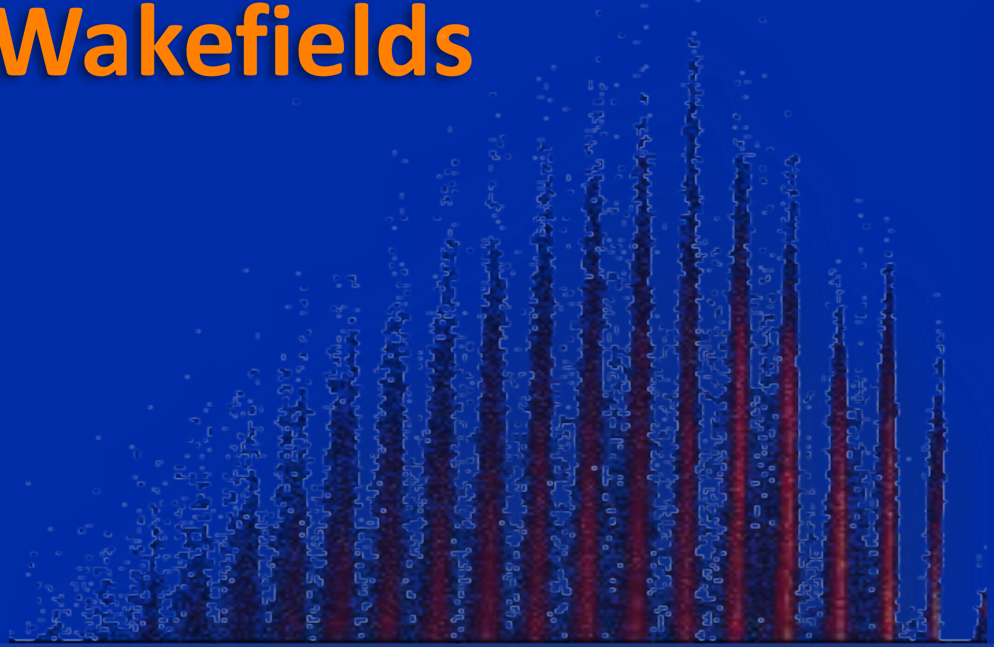

# Surface Plasmon (SP)

Plasma wave confined on surface

## Plasmon

A Quantum of Plasma Oscillation

Collective density oscillations of the free electron gas in a metal or semiconductor.

- A quantum: $\hbar\omega_p$
- Bulk or surface

## SP

Confined plasmon at **Interfaces**

Plasmon that exists at the interface between a metal and a dielectric material.

- **Confined**
- A quantum: $\hbar\omega_{sp} = \hbar\omega_p/\sqrt{2}$

## SPP

Surface plasmon polariton

An EM wave coupled with an SP propagates along the interface.

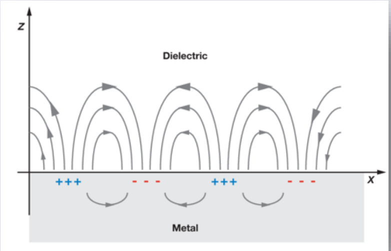


## LSP

Localized surface plasmon

Plasmon confined in a metallic nanoparticle or any small metallic structure.

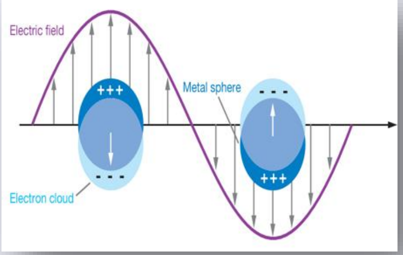

# Relativistic Surface Plasmon (RSP)

## A new regime to be discovered: Basic Equations of RSP

Maxwell's Equations

$$\nabla \cdot \boldsymbol{E} = 4\pi\rho, \qquad \nabla \times \boldsymbol{E} = -\frac{1}{c}\frac{\partial \boldsymbol{B}}{\partial t}$$

$$\nabla \cdot \boldsymbol{B} = 0, \qquad \nabla \times \boldsymbol{B} = \frac{4\pi}{c}\boldsymbol{J} + \frac{1}{c}\frac{\partial \boldsymbol{E}}{\partial t},$$

Continuity equation $$\frac{\partial n_e}{\partial t} + n_e \nabla \cdot \boldsymbol{v} = 0,$$

Relativistic cold fluid momentum equation

$$\gamma m_e(\partial_t + \boldsymbol{v} \cdot \nabla)\boldsymbol{v} = -e\left(\boldsymbol{E} + \frac{\boldsymbol{v}}{c} \times \boldsymbol{B}\right) + \boldsymbol{F}_{\text{ext}},$$

The drive $\boldsymbol{F}_{ext}$ determines how SP can be excited.

- Ponderomotive potential $U_p$ of a laser pulse : $\boldsymbol{F}_{ext} = -n_e \nabla U_p$ @B. Lei et al. PPCF 67 (2025) 065036
- Electric field of a laser pulse: $\boldsymbol{F}_{ext} = -e n_e E_L$ @B. Lei et al. PRL. 135, 205001 (2025)
- Electric field of a charged particle beam: $\boldsymbol{F}_{ext} = -2\,\pi e^2 n_b n_e r_b / \gamma_b^2 r$ @B. Lei et al NJP. 27 (2025) 084301

@ B. Lei et al. (2025) Book Chapter, ISBN: 978-1-83635-608-0 @ A new paper with more theoretical details is to be submitted.

# Wave equations with Ponderomotive Drive

## Linearization : Intrinsic VS. Drive

By assuming a small electron density perturbation $\delta n$ around the initial surface electron density $n_0$ and a sharp surface of stationary ion background, $n_C = n_0$. The current can be separated into two parts: the polarisation current $\boldsymbol{J}_{pol}$ and external source current $\boldsymbol{J}_{ext}$, as $\boldsymbol{J} = \boldsymbol{J}_{pol} + \boldsymbol{J}_{ext}$.

The linear plasma response in the frequency domain as

$$i\omega m_e \gamma_q (\boldsymbol{v}_{\mathrm{pol}} + \boldsymbol{v}_{\mathrm{ext}}) = e\boldsymbol{E} + \nabla U_p$$

As a result, the polarisation current is given by $$\boldsymbol{J}_{\mathrm{pol}} = -\frac{e^2 n_0}{i\omega m_e \gamma_q}\boldsymbol{E} = i\frac{\omega_p^2}{4\pi\omega\gamma_q}\boldsymbol{E},$$

The source drive current is given by $$\boldsymbol{J}_{\mathrm{ext}} = -en_0\boldsymbol{v}_{\mathrm{ext}} = i\frac{en_0}{\omega\gamma_q m_e}\nabla U_p.$$

Relativistic Drude permittivity:

$$\varepsilon(\omega) = 1 - \frac{\omega_p^2}{\boldsymbol{\gamma_q}\,\omega(\omega + i\nu)}$$

# Wave equations in General
## Helmholtz equation

From the Maxwell-Ampere equation

$$\boxed{\left(\nabla \times \nabla \times -\frac{\omega^2}{c^2}\varepsilon(\omega)\right)\boldsymbol{E} = \mathcal{L}(\omega)\boldsymbol{E} = i\frac{4\pi\omega}{c^2}\boldsymbol{J}_{\rm ext}}$$

Here $\mathcal{L}(\omega) = \nabla \times \nabla \times -\omega^2\varepsilon(\omega)/c^2$ is the vector Helmholtz operator.

The source term $\boldsymbol{S} = i\frac{4\pi\omega}{c^2}\boldsymbol{J}_{\rm ext} = -\frac{4\pi n_0 e}{\gamma_q m_e c^2}\nabla U_p$

The general solution

Eigen mode

$$\boxed{\boldsymbol{E}(\boldsymbol{r},t) \approx \underbrace{A(z,t)}_{\text{Envelope}}\boldsymbol{E}_{\rm sp}(\boldsymbol{r}_\perp)e^{i\zeta_{sp}} + c.c.,}$$

Since SPs are surface TM, the boundary conditions are

1) continuity of $E_\parallel$ and $B_\parallel$
2) $D_\perp = \varepsilon E_\perp$, which give the dispersion relation $D(\omega, k) = 0$.

# Wave equations in General

## Eigen modes

Eigen modes

$$\boxed{\mathcal{L}(\omega_{\rm sp})\boldsymbol{E}_{sp} = 0}$$

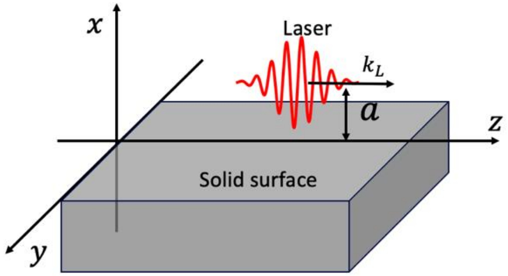


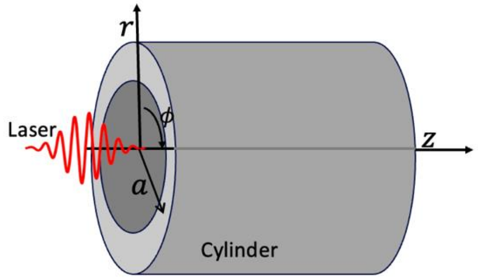


- It is intrinsic to the nature of SP
- Determines the dispersion relation
- The exact form depends surface geometry.

- Planar surface

Vacuum $$E^{(1)}_{{\rm sp},z}(x) = E_{{\rm sp},0}e^{-\kappa_1 x}e^{i\zeta_{\rm sp}}$$

Plasma $$E^{(2)}_{{\rm sp},z}(x) = E_{{\rm sp},0}\frac{\kappa_1}{\kappa_2}e^{\kappa_2 x}e^{i\zeta_{\rm sp}},$$

- Cylindrical surface

$$E^{(1)}_{{\rm sp},z,m}(r,\phi,z) = E_{{\rm sp},0}I_m(\kappa_1 r)e^{im\phi+i\zeta_{\rm sp}}$$

$$E^{(2)}_{{\rm sp},z,m}(r,\phi,z) = E_{{\rm sp},0}\frac{I_m(\kappa_1 a)}{K_m(\kappa_2 a)}K_m(\kappa_2 r)e^{im\phi+i\zeta_{\rm sp}}$$

# Field Envelope in General

## With SVEA for ponderomotive drive

By assuming a slowly varying envelope (SVEA), $|\partial_z A| \ll k_{sp}|A|$, and $|\partial_t A| \ll \omega_{sp}|A|$

Envelope equation

$$\boxed{(\partial_t + v_g \partial_z + \Gamma)A = \frac{i\omega_{\text{sp}}}{2\mathcal{N}} \int d\mathbb{A}\, \boldsymbol{E}^*_{\text{sp}} \cdot \boldsymbol{J}_{\text{ext}}.}$$

For ultrashort laser drive:

$$\boxed{(\partial_t^2 + 2\Gamma\partial_t + \omega_{\text{sp}}^2 - v_g^2\partial_z^2)A(z,t) \approx \frac{i\omega_{sp}^2}{\mathcal{N}} \Re\left\{ \int d\mathbb{A}\, \boldsymbol{E}^* \cdot \boldsymbol{J}_{\text{ext}} \right\}}$$

With Brillouin energy moralization:

$$\mathcal{N} = \frac{1}{16\pi} \int \left( |\boldsymbol{B}_{sp}|^2 + \Re\{\partial_\omega(\omega\varepsilon)\}|\boldsymbol{E}_{sp}|^2 \right) d\mathbb{A}$$

- The general solution of the wakefield can be obtained by Green's method.
- The exact form of the solution depends on the surface geometry.

# Geometric Effects

## @ 3D PIC simulations

Planar surface

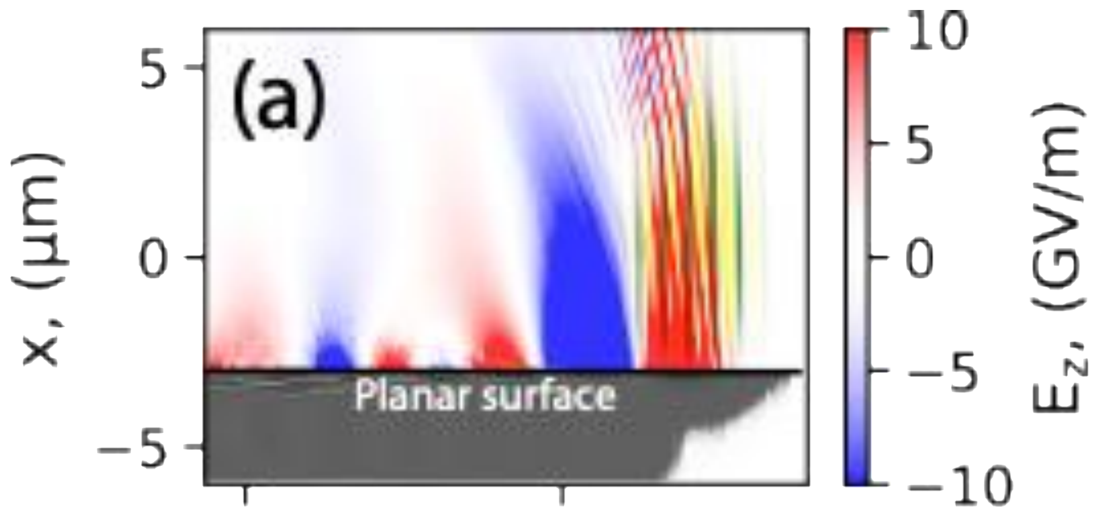


Cylinder surface

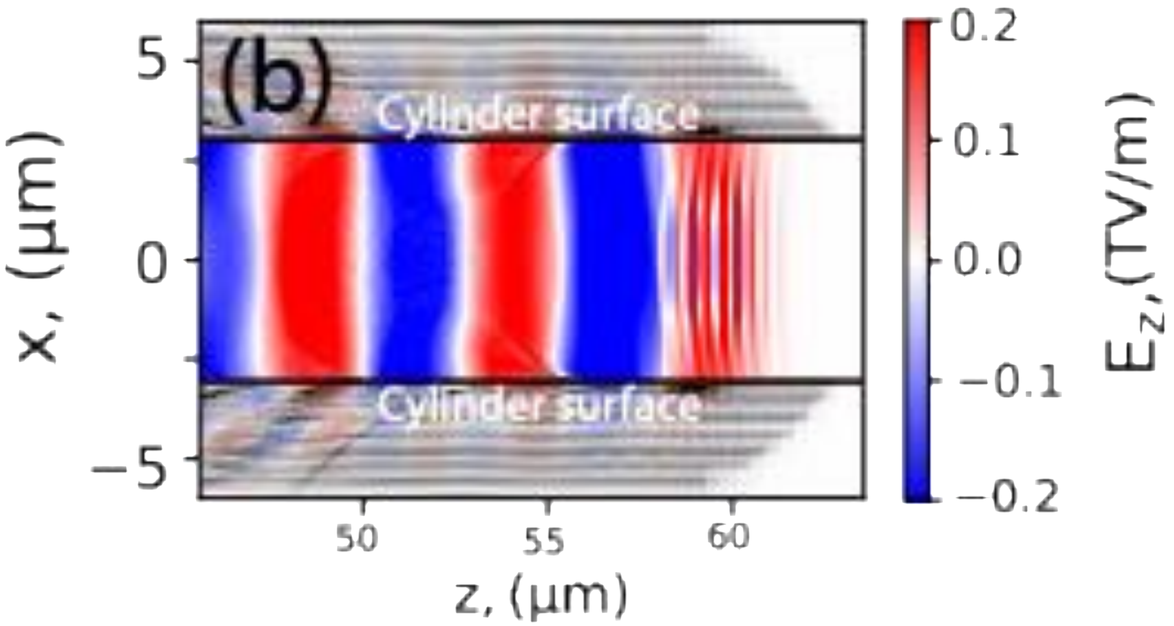

# Relativistic Effects

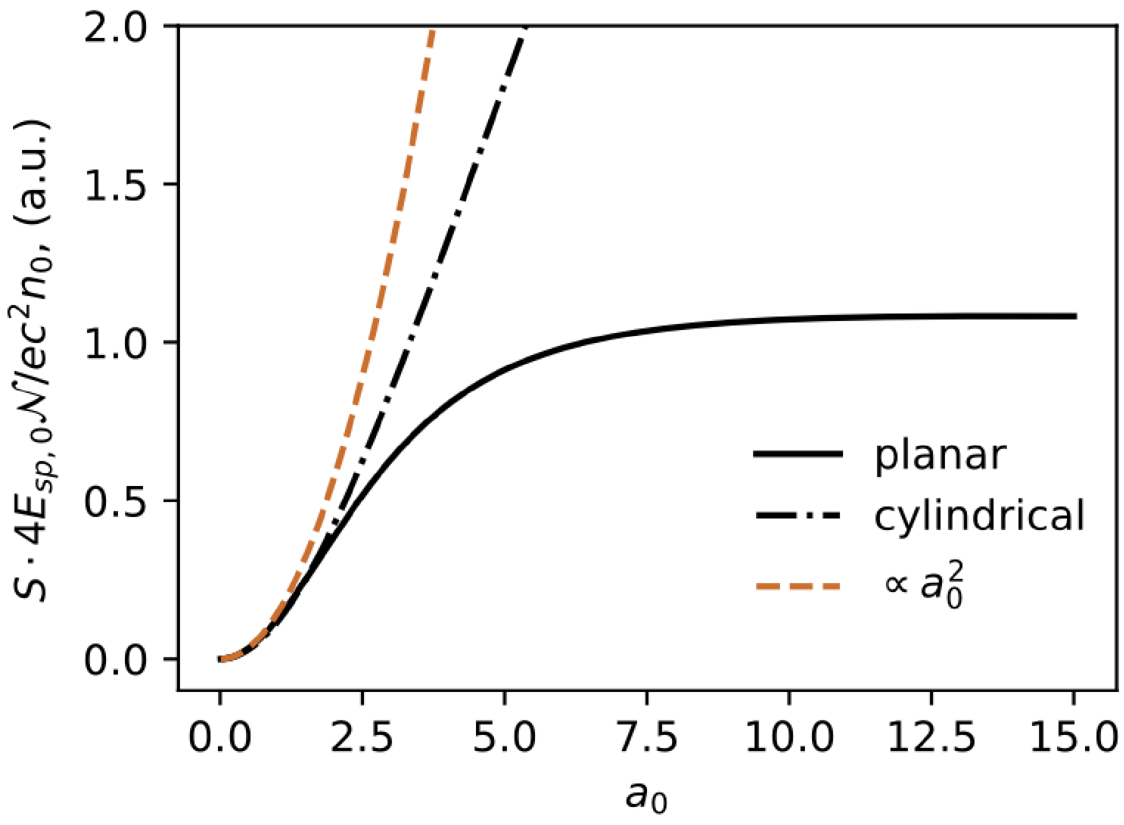


- Field saturates due to relativistic effects on planar surface.
- Field saturation is significantly mitigated by curved surface, promising feature for high-intensity drive.
- **However**, with higher $a_0$, the sharp surface condition fails, and the field needs to be modified.

# Wave equations in General

## Dispersion relation and relativistic effects

- Planar surface

$$\frac{\kappa_1}{\varepsilon_1} + \frac{\kappa_2}{\varepsilon_2} = 0,$$

- Cylindrical surface

$$\frac{\varepsilon_1}{\kappa_1}\frac{I'_m(\kappa_1 a)}{I_m(\kappa_1 a)} + \frac{\varepsilon_2}{\kappa_2}\frac{K'_m(\kappa_2 a)}{K_m(\kappa_2 a)} = 0,$$

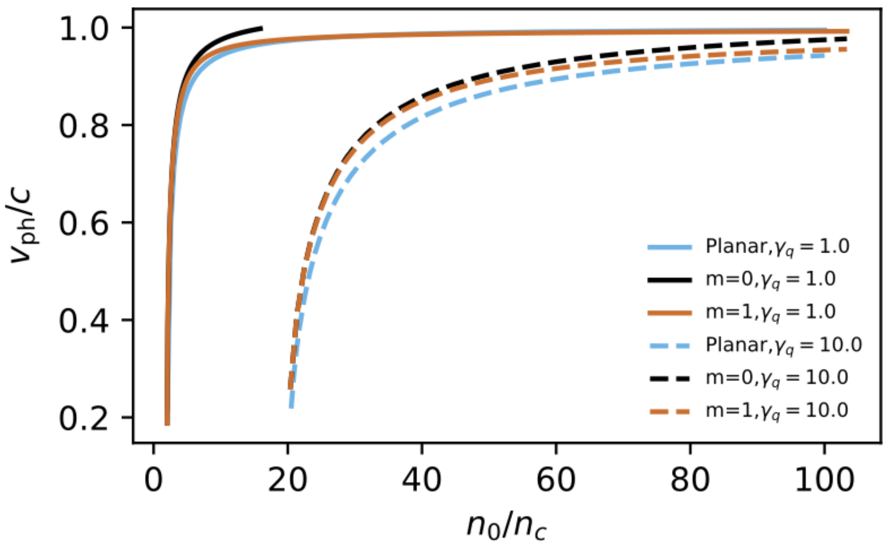


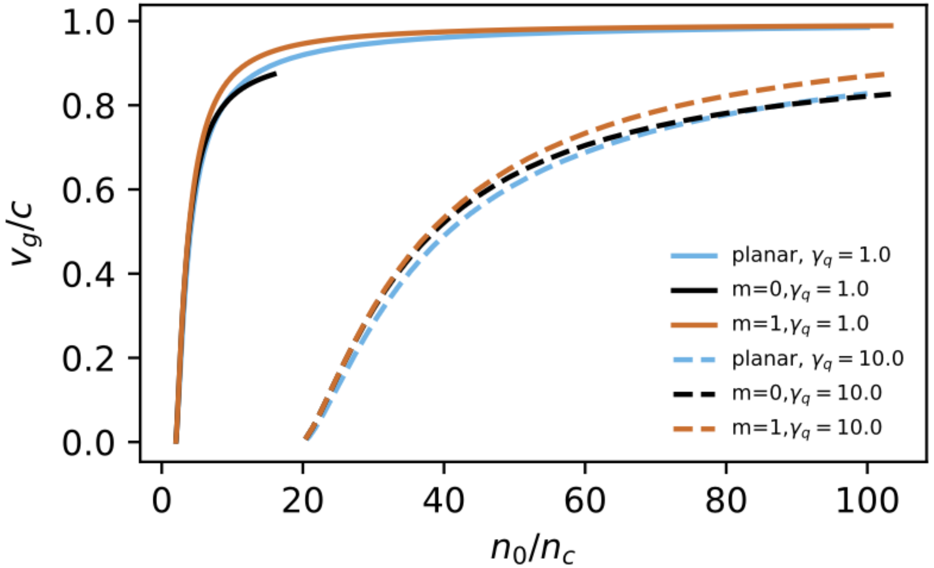

# Sharp Surface Threshold

When the front of the laser pulse arrives, the surface electrons are expelled outwards by the laser ponderomotive potential and pulled back by the bulk plasma to form an electron layer of spatial density profile, which is experienced by the main pulse. Assuming this process is adiabatic, the equilibrium condition of the surface is

$$\boxed{U_p^{\mathrm{surf}} \geq e\Phi_b,}$$

The electron escape condition

$$a_0 > \sqrt{\frac{3}{s\eta}}.$$

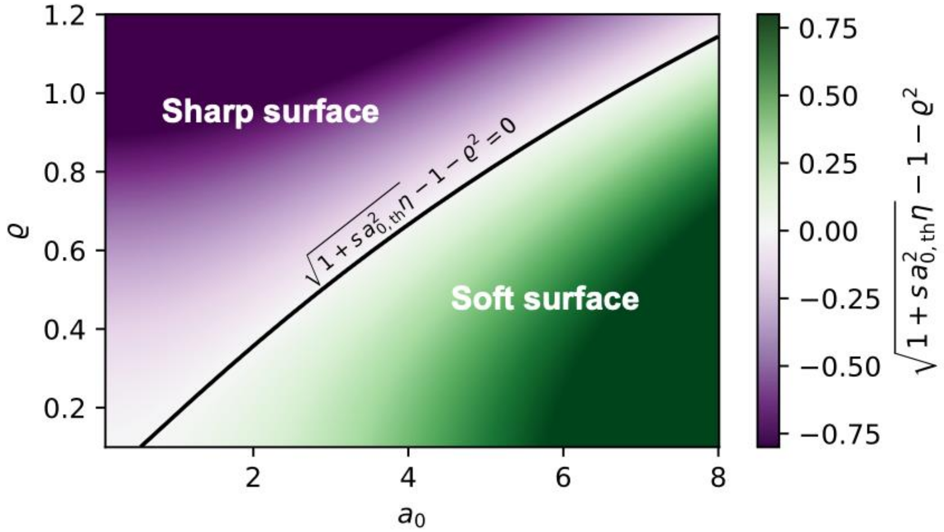


| $\lambda_L$ | $n_e$ | $w_0$ | $a_{0,th}$ | $I_{0,th}$ |
|---|---|---|---|---|
| $0.8\ \mu m$ | $10^{22}\ cm^{-3}$ | $2.0\ \mu m$ | 9.3 | $2.0 \times 10^{20} W \cdot cm^{-2}$ |

@C. Riconda et al. POP 22, 073103 (2015).
@B. Lei et al. PPCF 67 (2025) 065036

# Pre-plasma Effects

Pre-plasma effects can be studied by introducing a soft plasma layer on the surface. The wave equation on sharp surface is modified as

- On planar surface

$$\frac{d}{dx}\left(\frac{1}{\varepsilon}\frac{dE_z}{dx}\right)+\left(\frac{k^2}{\varepsilon}-\frac{\omega^2}{c^2}\right)E_z=S_z^{(x)}(x;\omega,k),$$

- On cylindrical surface

$$\frac{1}{r}\frac{d}{dr}\left(\frac{r}{\varepsilon}\frac{dE_z}{dr}\right)+\left(\frac{k^2}{\varepsilon}-\frac{\omega^2}{c^2}-\frac{m^2}{\varepsilon r^2}\right)E_z=S_z^{(r)}(r;\omega,k)$$

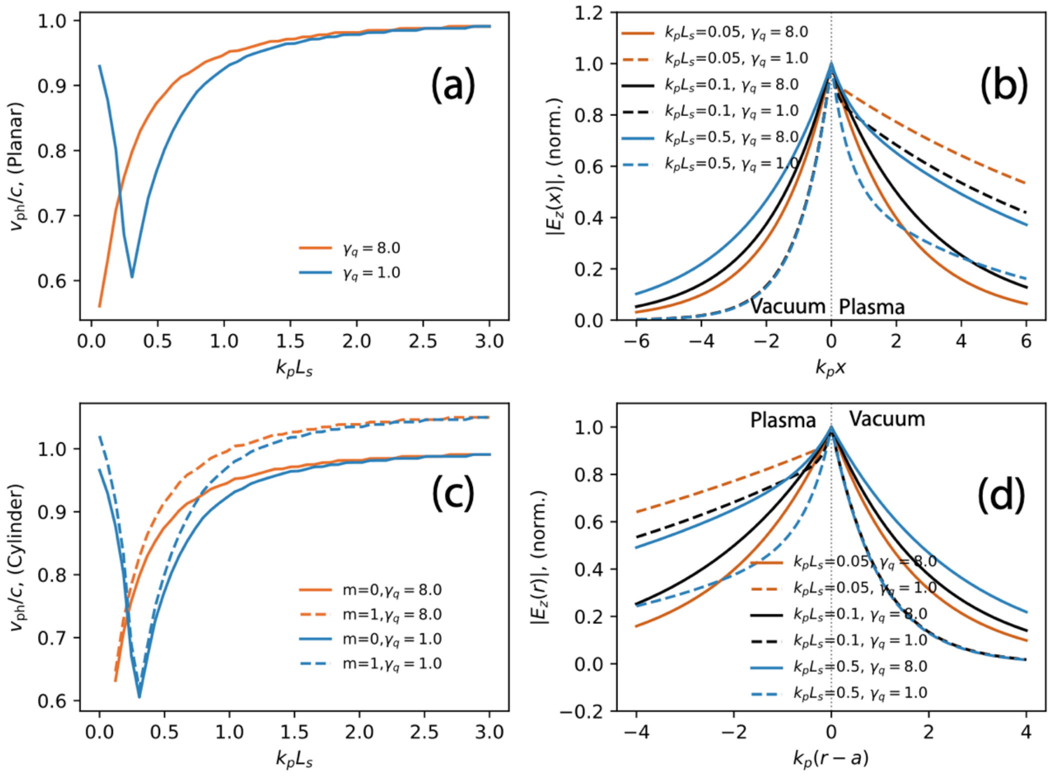


The dispersions are also modified.

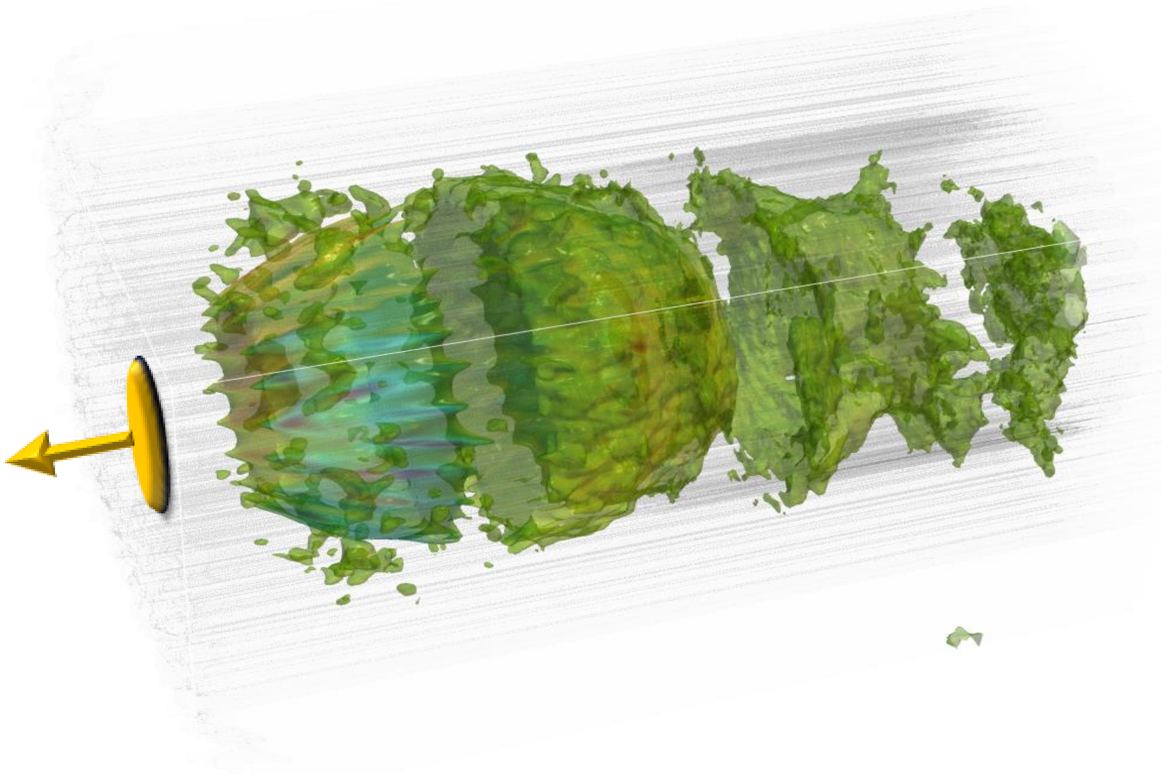

# RSP-based wakefield acceleration

- Photon VS. Particle Driver
- Leaky VS. bubble wakefield
- Electron VS. Positron Acceleration

# Leaky Field Acceleration on Sharp Surface

## Electron Beam-driven on CNT microtube

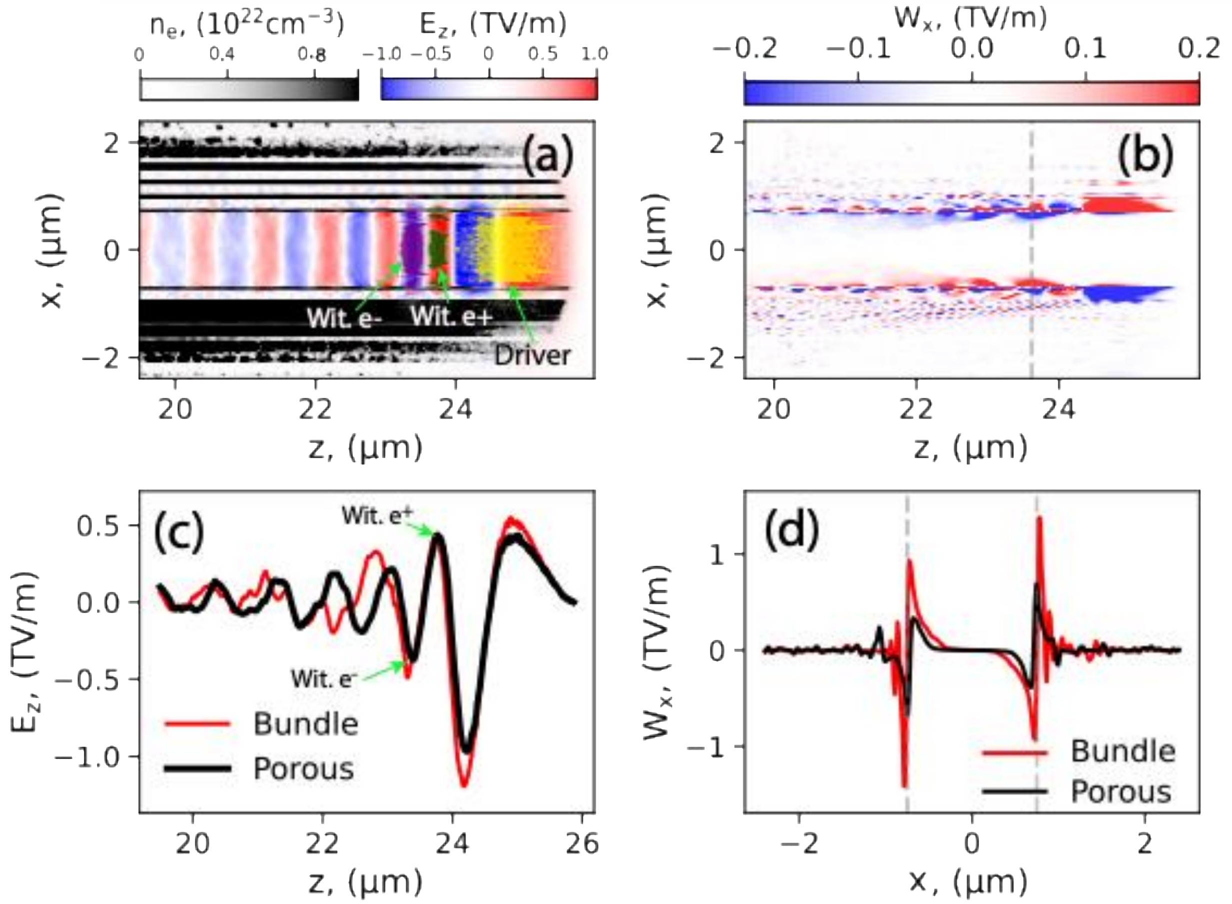


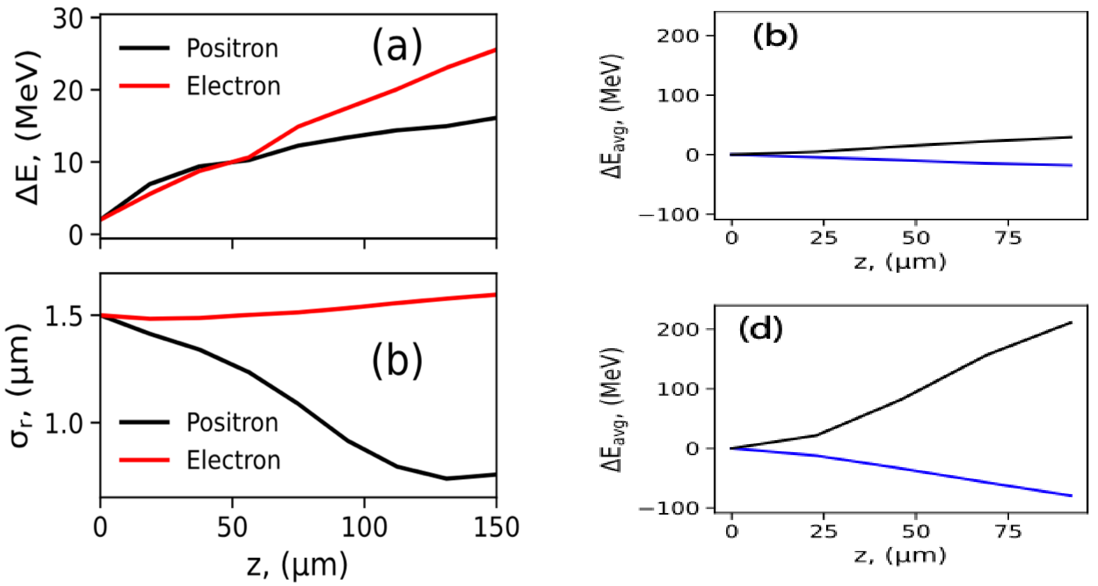


- Both are capable of accelerating electrons and positrons
- Acceleration gradient to several TeV/m-level

@B. Lei et al. PPCF 67 (2025) 065036
@B. Lei et al NJP. 27 (2025) 084301

@3D PIC by WarpX

# Bubble Wakefield Acceleration on Soft Surface

## Laser & beam-driven on CNT microtube

### Laser-driven

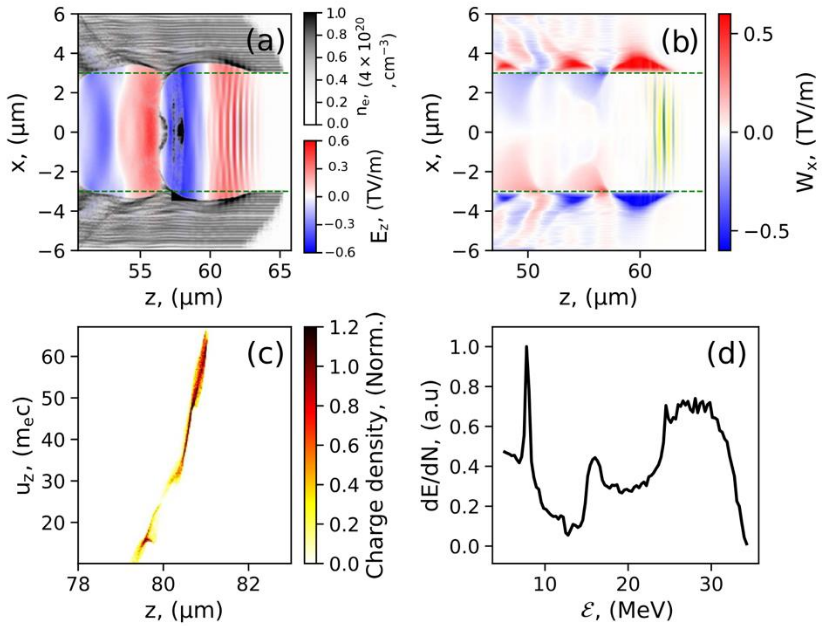

- Bubble wakefield is similar to gaseous plasma
- Up to 100s TV/m field strength

### Electron beam-driven

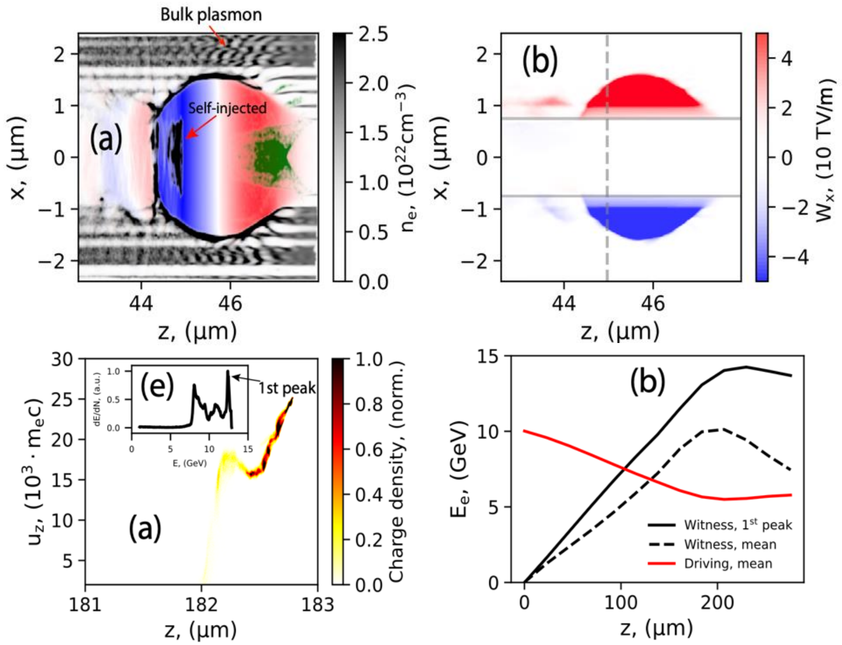


- Self-injection possible, $\eta > 60\%$
- Capable of electron and positron acceleration

# RSP-based Coherent Synchrotron Radiation (CSR) Emission

**A new way to ultra-compact coherent source**

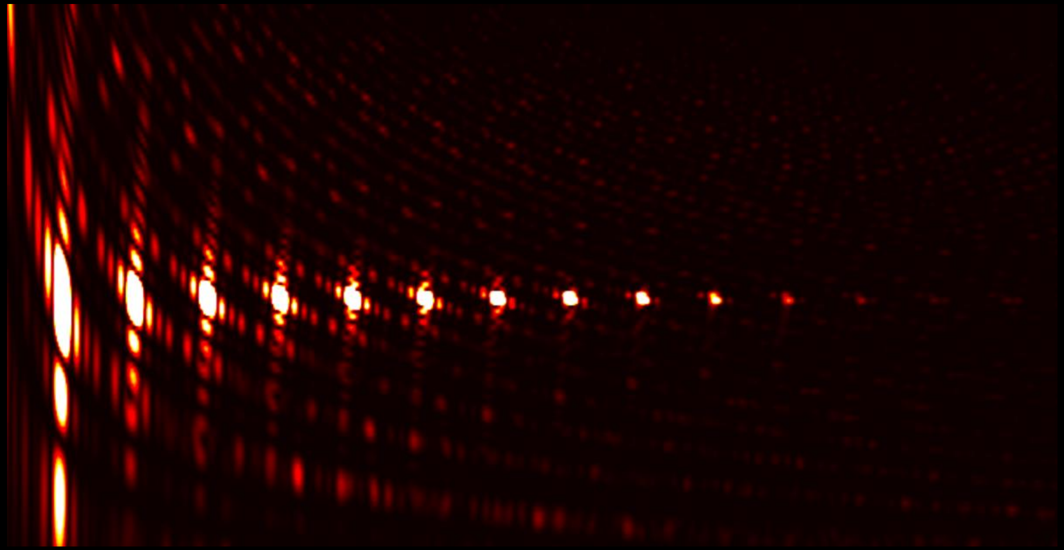

# SPP Excitation by CP Laser

The SPP excitation can be described by our RSP theory.

$$\left(\nabla\times\nabla\times-\frac{\omega^2}{c^2}\varepsilon(\omega)\right)\boldsymbol{E}=\mathcal{L}(\omega)\boldsymbol{E}=i\frac{4\pi\omega}{c^2}\boldsymbol{J}_{\mathrm{ext}}$$

The general solution

Eigen mode : field shape

$$\boldsymbol{E}(\boldsymbol{r},t)\approx\boxed{A(z,t)}\boxed{\boldsymbol{E}_{\mathrm{sp}}(\boldsymbol{r}_\perp)}e^{i\zeta_{sp}}+c.c.,$$

Envelope: amplitude

Coupling efficiency is determined by the eigen modes

$$\mathcal{L}(\omega_{\mathrm{sp}})\boldsymbol{E}_{sp}=0$$

@B. Lei et al. PRL. (2025) Accepted, preprint: arXiv:2507.04561

In vacuum region, $r < a$: $\epsilon = \epsilon_v = 1$ and $\kappa_1^2 = k_z^2 - \omega^2/c^2$. We need fields finite at $r = 0$, so we choose $I_m$ and the z-component is written as

$$E_{z1}(r) = A\, I_m(\kappa_1 r)$$

and $$B_{z1}(r) = B\, I_m(\kappa_1 r)$$

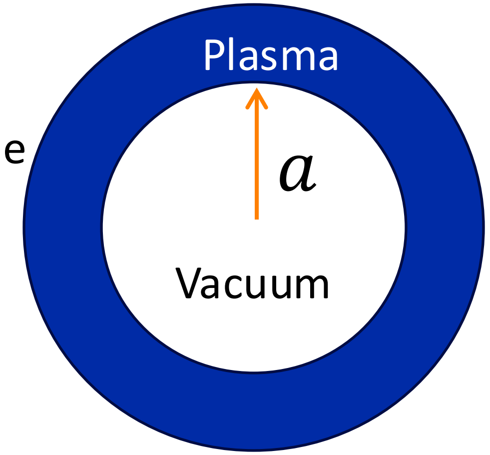


In plasma region, $r > a$: $\epsilon = \epsilon_p = 1 - \omega_p^2/\omega^2$. For solid plasma, $\omega < \omega_p$, so $\epsilon_p < 0$ and $\kappa_2^2 = k_z^2 - \omega^2\epsilon_p/c^2$ Since $\epsilon_p < 0$ , $\kappa_2^2$ is always positive for real $k_z$. Here, we need fields decay to zero as $r \to \infty$, so the field can be written as

$$E_{z2}(r) = C\, K_m(\kappa_2 r) \text{ and } B_{z2}(r) = D\, K_m(\kappa_2 r)$$

# Cylindrical Mode Selection

Coupling efficiency

$$A \propto \int_0^a \int_0^{2\pi} \left(\mathbf{E}_{spp,\perp} \cdot \mathbf{E}^*_{laser,\perp}\right)\Big|_{z=0} r\,dr\,d\phi,$$

With a laser driver of azimuthal dependence $e^{il\phi}$

$$(\mathbf{E}_{spp}^{(m)} \propto e^{im\phi})\cdot(\mathbf{E}^*_{\mathrm{laser}} \propto e^{-il\phi}) \sim e^{im\phi} \times e^{-il\phi} = e^{i(m-l)\phi}$$

- The matched mode $m = l$ can efficiently excite the corresponding mode.
- CP laser -- > $m = 1$ mode
- Higher-order mode is also possible, e.g. LG.

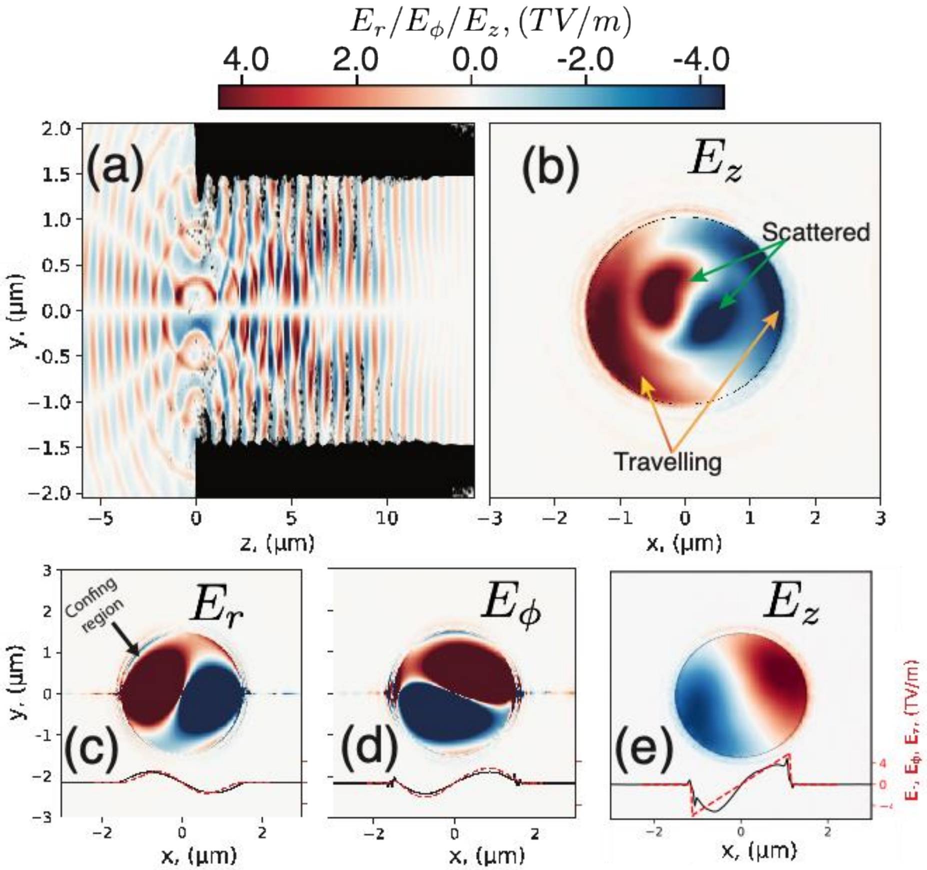

# Direct Electron Acceleration and Modulation

## Superluminal quasi-particle

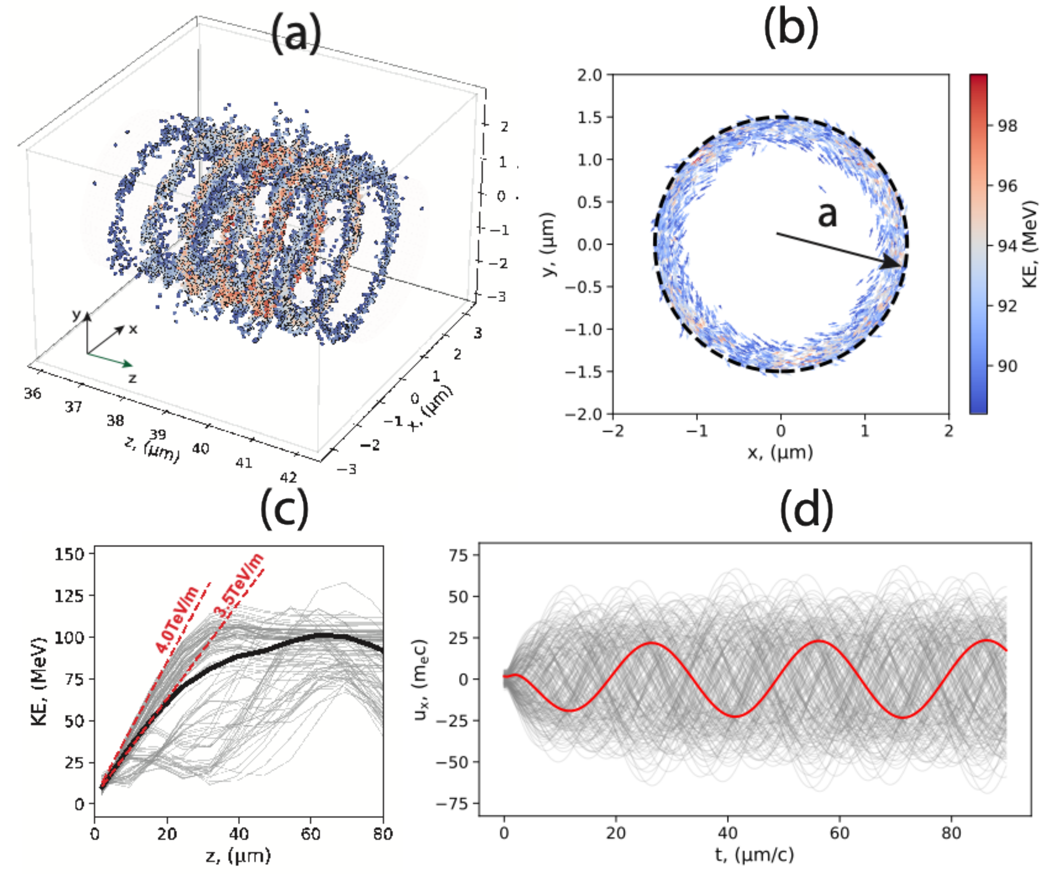


Surface electrons can be trapped, accelerated and modulated in SPP field.

- Stable propagation for several Rayleigh lengths.
- Acceleration gradient: 4.0 TeV/m in peak
- High charge: 18.7 pC@>90MeV
- Helical modulation: $\omega_r = \sqrt{e(E_\phi + \beta_z c B_r)/m_e a}$
- Superluminal quasi-particle: $\beta_{ph} \simeq 1/\left(1 - \frac{\omega_r}{\omega_m}\right) > 1$

# CSR Emission

## Optical shock in Vavilov-Cherenkov angle

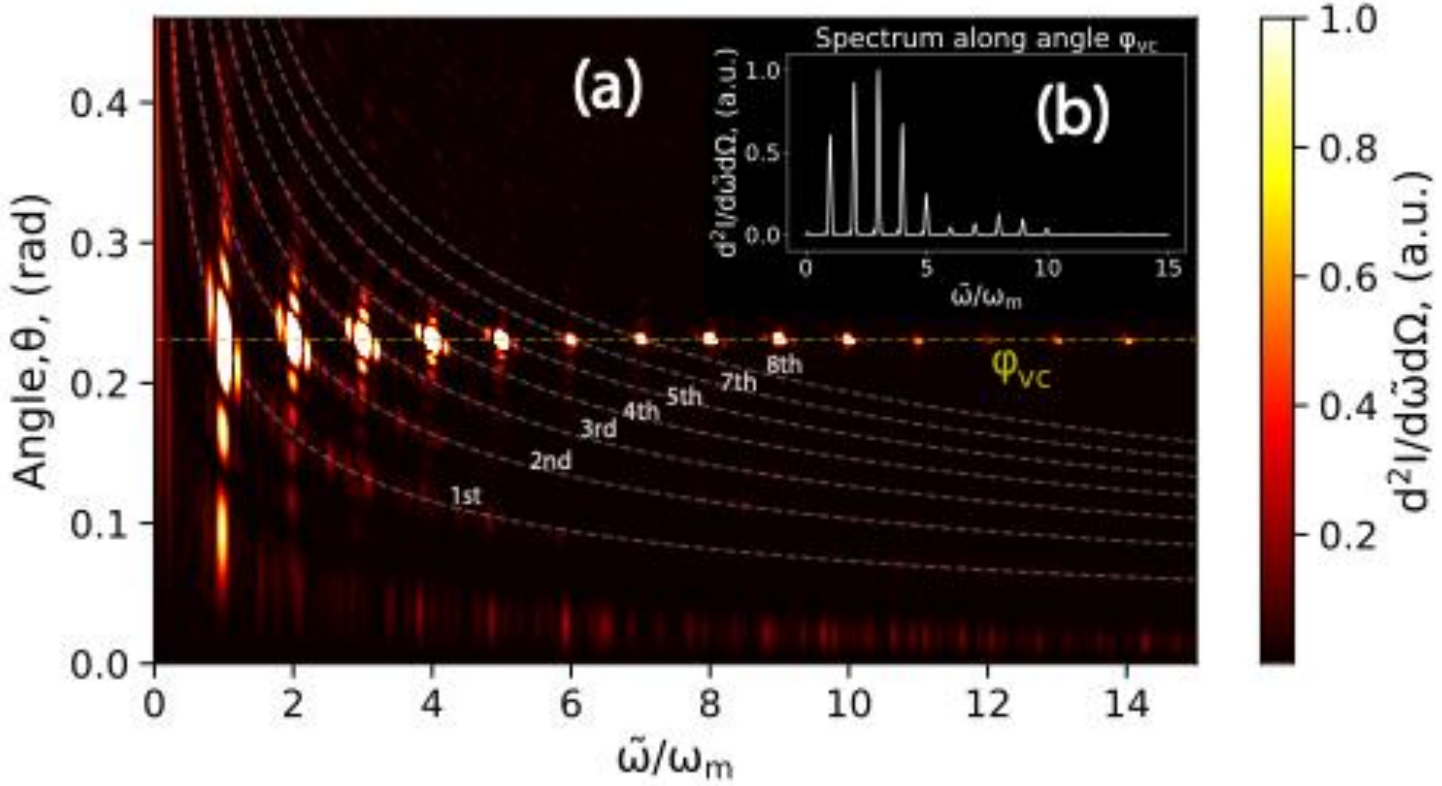


CSR emission along VC angle in the form of optical shock at the harmonics of the modulation frequency.

This is the first viable solution to generate the generalized superradiance.

# CSR Emission with Azimuthal Symmetry

## Beyond state-of-the-art

Helical trajectory of an electron $j$

$$\boldsymbol{r}_j = (x_j, y_j, z_j) = \frac{r_{0,j}}{2}\left(\boldsymbol{\epsilon} e^{i\omega_r t + i\psi_j} + c.c.\right) + \boldsymbol{\eta}\beta_{z,j} ct$$

Azimuthal symmetry of electron beam

$$\psi_j = \frac{2\,\pi j}{N}$$

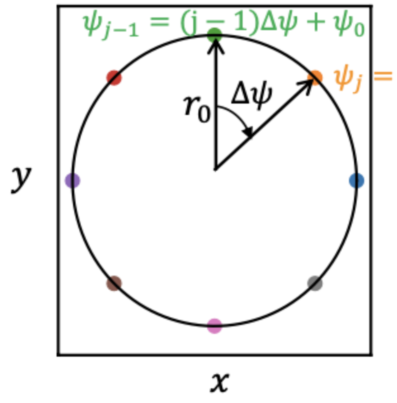


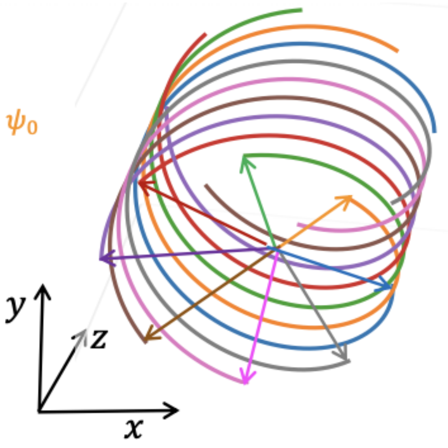


Radiation intensity:

$$dI/d\omega\, d\Omega = I_0|\boldsymbol{A}|^2 \propto N^2$$

With central frequency of harmonic :

$$\tilde{\omega}_n = (nN \pm 1)\omega_r/(1 - \beta_z \cos\theta \sin\phi)$$

- We can generate high-flux per electron CSR
- The coherent radiation can be in arbitrary angle, such as on-axis
- The harmonics can be well separated.

# CSR Emission with Azimuthal Symmetry

## On-axis spectrum & isolated Harmonics

Isolated harmonics

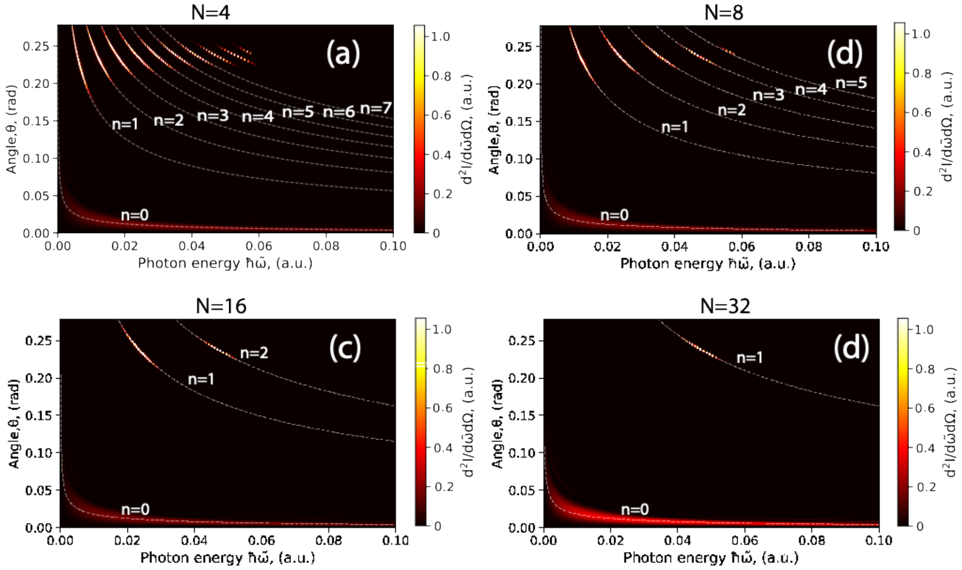


On –axis CSR

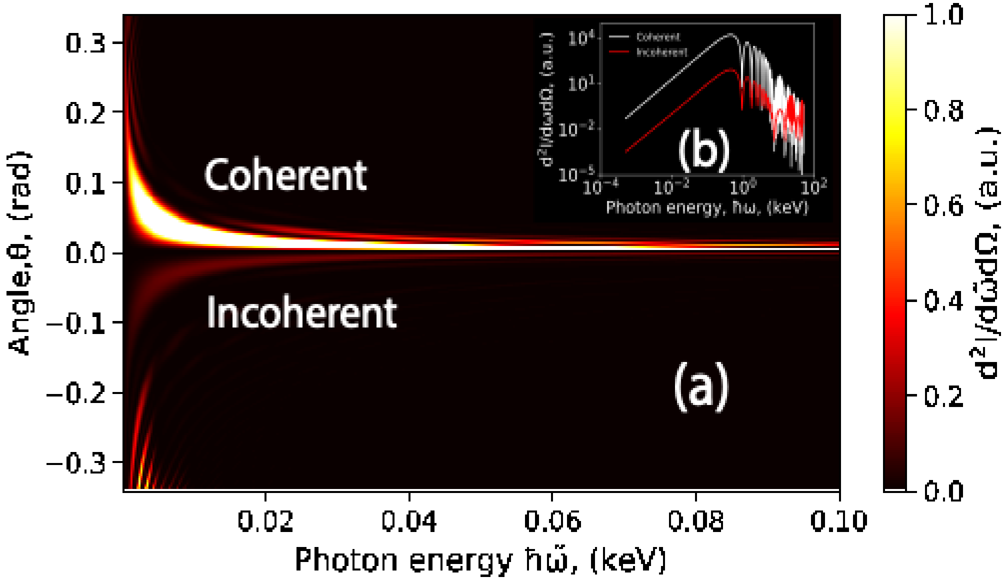

# Significances and Summary

| Physical qualities | Our CSR | FEL |
|---|---|---|
| **Emission angle** | • In general case, our source emits radiation into a conical shell at a specific off-axis Vavilov-Cherenkov angle.<br>• In the special case where the electrons distribution inside the beam is azimuthally uniform, the on-axis radiation can also be coherent. | • FELs produce an extremely bright, narrow cone of radiation directed on-axis, with a typical divergence angle of $1/\gamma$. |
| **Spectrum** | • Our mechanism, arising from a wiggler-like helical motion, naturally produces broadband, coherent radiation composed of multiple, well-defined harmonics, as seen in Figure 4(b) in the revised manuscript.<br>• This is a characteristic feature of generalized superradiance in the wiggler regime.<br>• A broadband, coherent source could be highly valuable for applications requiring multi-spectral probes or generating attosecond pulses. | • FELs are fundamentally narrow-band sources.<br>• Such radiation is ideal for resonant spectroscopy and diffraction imaging. |
| **Beam requirements** | • Our scheme is far more tolerant to variations in electron beam quality, such as energy spread. | • FELs requires high-quality beam, e.g. micro bunching, low energy spread, etc. |
| **Compactness** | • our scheme is extreme compact. The entire radiation generation process occurs over tens of micrometers within a plasma structure. | • FELs require large-scale accelerators and undulators that are up to tens of hundreds of meters long. |

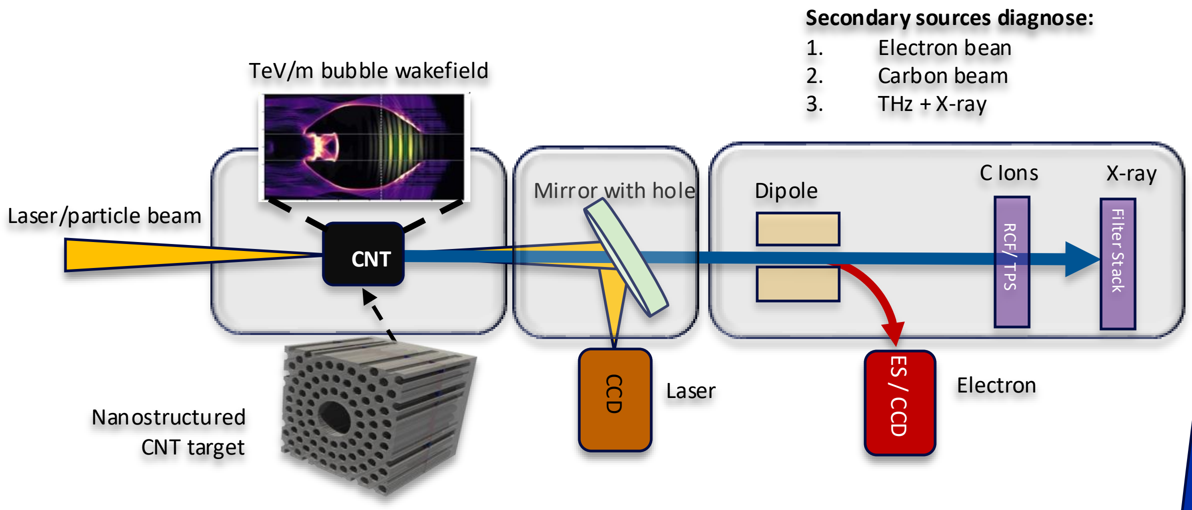


# Experimental feasibility and opportunities

# Target : Nano-structured CNTs

## CNTs in dense forest form

**@Hung et al APL 91, 093121 (2017)**

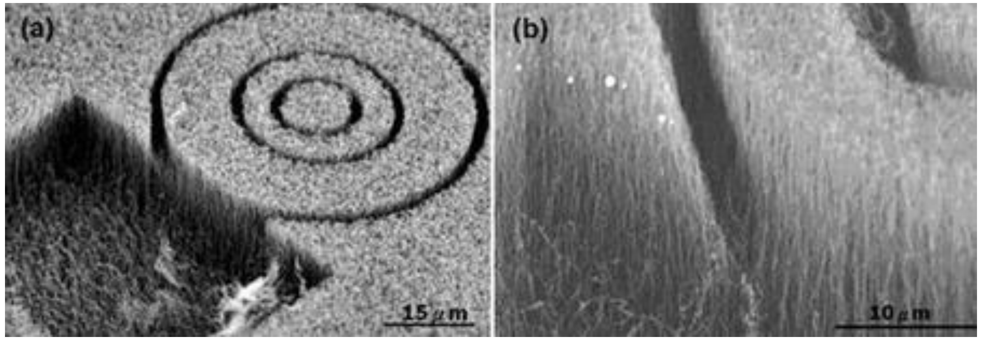


**@Teen et al nano express, 579 (2012)**

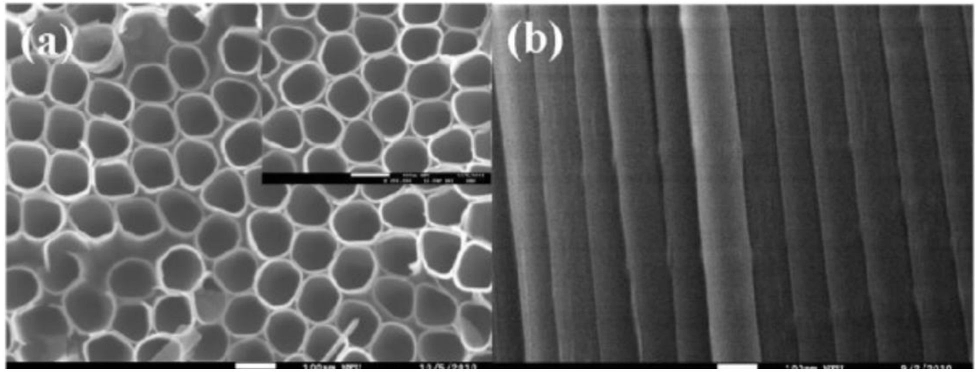


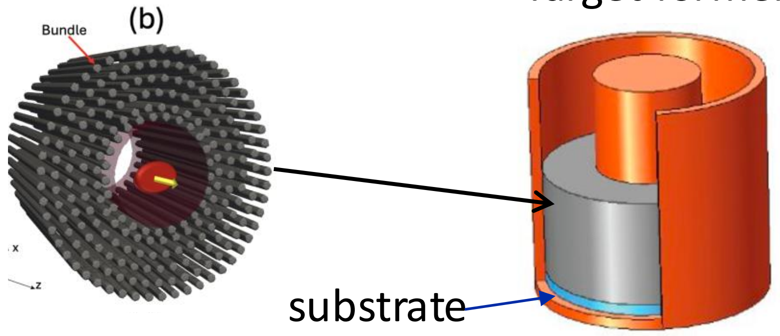


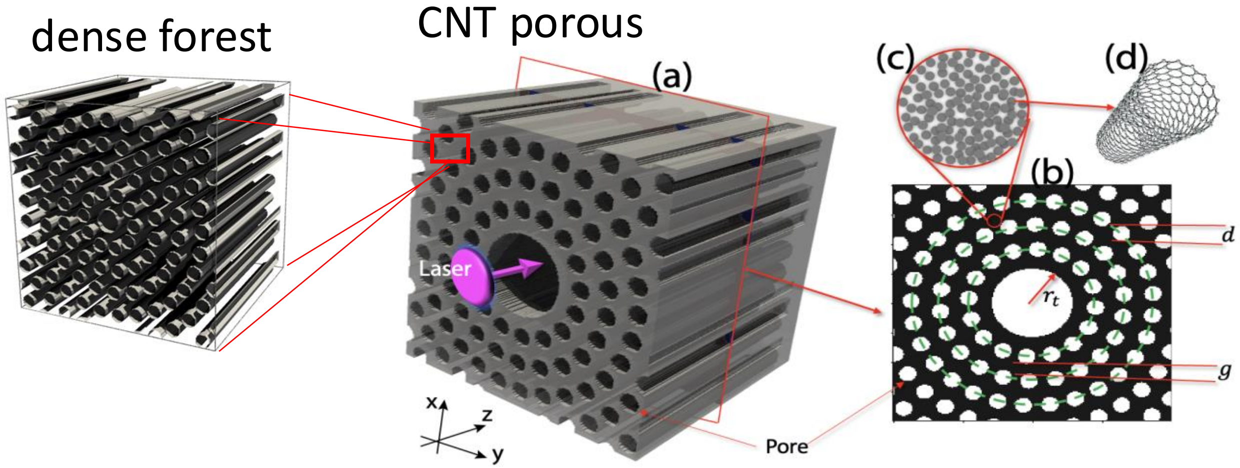

# Target : Solid Plasma Micro-Channel

## With great flexibility

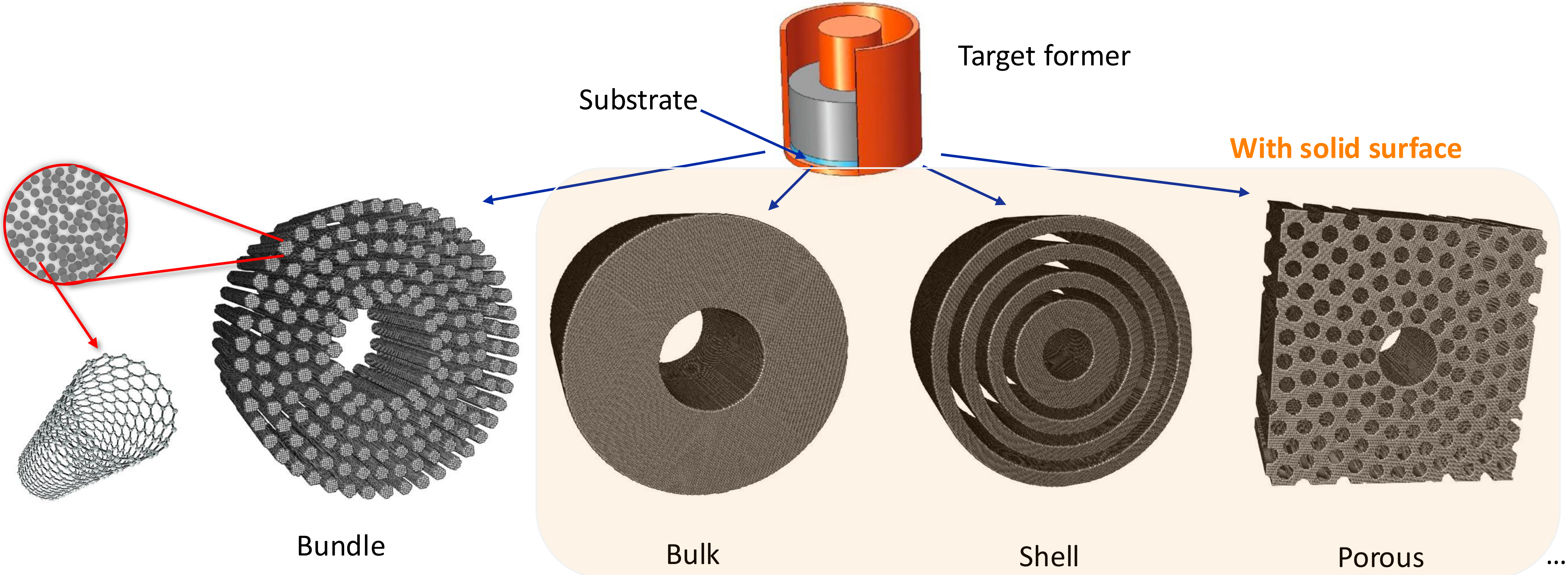

# Laser facilities

| | FEBE @STFC, UK | Jeti200 @HIJ, DE | SCAPA @UOS, UK | POLARIS @HIJ, DE | Vega-II @CLPU, ES | Vulcan @CLF, UK | SULF @SIOM, CN | ALPS @ELI, HU |
|---|---|---|---|---|---|---|---|---|
| Peak power | 120 TW | 200 TW | > 350 TW | 200 TW | 200 TW | 1 –> 20 PW | **10 PW** | 2 PW |
| Intensity | $\sim 10^{19}$ | $>10^{21}$ | $\sim 10^{21}$ | $> 10^{21}$ | $\sim 10^{20}$ | $\sim 10^{21}$ | $> 10^{22}$ | $10^{22}$ |
| Polarization | LP | LP | LP | LP | LP | LP | LP | LP |
| On-target Energy | 2.7 J | 4-5.6 J | 8.75 J | 17 J | 4-7 J | 500 J | 70 J | 34 J |
| Duration | < 23fs | < 17 fs | 25 fs | **<100 fs** | 30 fs | 500 fs | 20 fs | < 20 fs |
| Tem. contrast | $10^{-6}$ | $10^{-13}$ | $10^{-10}$ | $\mathbf{10^{-13}}$ | $10^{-10}$ | $10^{-10}$ | $10^{-11}$ | $10^{-11}$ |
| Ponting Jitter | < 5 $\mu rad$ | $\sim 2\ \mu rad$ | < 5 $\mu rad$ | | | | | < 10 $\mu rad$ |

# Beam facilities

| | | FACET-II $e^-$ beam @SLAC, US | FACET-II $e^+$ beam @SLAC, US | CLARA $e^-$ beam @SFTC, UK | XFEL @DESY, DE | SXFEL/SHINE @SSRF, CN |
|---|---|---|---|---|---|---|
| Energy | | 10 [4.0-13.5] GeV | 10 [13] GeV | 0.25 GeV | 17.5 GeV | 1.5 GeV / 8 GeV |
| Charge | | 2 [0.5-5] nC | 1 nC | 0.25 [0.02-0.25] nC | 1 nC | 0.5 nC / 100 pC |
| Peak current | | 300 kA | 20 kA | 1-3 kA | 5 kA | > 1kA / > 1.5 kA |
| Beam size | x | 3 um | 3 um | 10 um | 16 um | 100 um / 22 um |
| | y | 2 um | 2 um, | 10 um | 16 um | 100 um / 22 um |
| | z | 0.48 um | 0.48 um | 9/30 um | 24 um | 6.9 um / 6 um |
| Max. beam density | | **1e24 c.c.** | **1e24 c.c.** | 1e16 c.c. | ~1e17 c.c. | ~1e14 c.c. / 1e16 c.c. |
| Min. energy spread, % | | 1.4 [0.4-1.6] | 0.1 | 0.01-0.06 | 0.012 % | < 0.02 % / < 0.01 % |

# Challenges

## Towards to Proof-of-Principle

### Theory

- Self-consistent framework
- Fundamental of end-coupling mechanism
- Nonlinear wakefield and electron trapping
- Geometric effects
- Relativistic effects
- Strong field effects, e.g. QED
- …

### Simulation

- Accuracy VS. Performance
- Nano structures modelling
- Materials properties
- Hydrodynamics
- Radiation calculation
- Classical VS. Quantum VS. Fluid VS. Atomic
- Parameters optimisation
- …

### Experiment

- Target fabrication
- Laser-target alignment
- Laser / beam qualities
- Target expansion and survivability
- High repetition rate
- Laser jitter
- …

# Thank you for your attention!

**Any questions?**

**Thanks to :** Hao Zhang, Alexandre Bonatto, Pablo Martin-Luna, Bin Liu, Daniel Seipt, Javier Resta-Lopez, Guoxing Xia, Qiao Bin, and Carsten Welsch

# Backups

# SPP Excitation by CP Laser

## Transverse Components

The transverse components are found from the axial components using Maxwell's equations:

$$E_{r,j} = -\frac{i}{\kappa_j^2}\left(k_z \frac{\partial E_{z,j}}{\partial r} + \frac{\omega m}{cr} B_{z,j}\right)$$

$$E_{\phi,j} = -\frac{i}{\kappa_j^2}\left(\frac{k_z m}{r} E_{z,j} - \frac{\omega}{c}\frac{\partial B_{z,j}}{\partial r}\right)$$

$$B_{r,j} = -\frac{i}{\kappa_j^2}\left(k_z \frac{\partial B_{z,j}}{\partial r} - \frac{\omega \epsilon_j m}{cr} E_{z,j}\right)$$

$$B_{\phi,j} = -\frac{i}{\kappa_j^2}\left(\frac{k_z m}{r} B_{z,j} + \frac{\omega \epsilon_j}{c}\frac{\partial E_{z,j}}{\partial r}\right),$$

**In vacuum**

$$E_{z1} = AI_m(\kappa_1 r)$$

$$B_{z1} = BI_m(\kappa_1 r)$$

$$E_{r1} = -\frac{i}{\kappa_1^2}\left(k_z A\kappa_1 I_m'(\kappa_1 r) + \frac{\omega m}{cr} BI_m(\kappa_1 r)\right)$$

$$E_{\phi 1} = -\frac{i}{\kappa_1^2}\left(\frac{k_z m}{r} AI_m(\kappa_1 r) - \frac{\omega}{c} B\kappa_1 I_m'(\kappa_1 r)\right)$$

$$B_{r1} = -\frac{i}{\kappa_1^2}\left(k_z B\kappa_1 I_m'(\kappa_1 r) - \frac{\omega m}{cr} AI_m(\kappa_1 r)\right)$$

$$B_{\phi 1} = -\frac{i}{\kappa_1^2}\left(\frac{k_z m}{r} BI_m(\kappa_1 r) + \frac{\omega}{c} A\kappa_1 I_m'(\kappa_1 r)\right)$$

**In plasma**

$$E_{z2} = CK_m(\kappa_2 r)$$

$$B_{z2} = DK_m(\kappa_2 r)$$

$$E_{r2} = -\frac{i}{\kappa_2^2}\left(k_z C\kappa_2 K_m'(\kappa_2 r) + \frac{\omega m}{cr} DK_m(\kappa_2 r)\right)$$

$$E_{\phi 2} = -\frac{i}{\kappa_2^2}\left(\frac{k_z m}{r} CK_m(\kappa_2 r) - \frac{\omega}{c} D\kappa_2 K_m'(\kappa_2 r)\right)$$

$$B_{r2} = -\frac{i}{\kappa_2^2}\left(k_z D\kappa_2 K_m'(\kappa_2 r) - \frac{\omega \epsilon_p m}{cr} CK_m(\kappa_2 r)\right)$$

$$B_{\phi 2} = -\frac{i}{\kappa_2^2}\left(\frac{k_z m}{r} DK_m(\kappa_2 r) + \frac{\omega \epsilon_p}{c} C\kappa_2 K_m'(\kappa_2 r)\right)$$

Be noted that the common factor $e^{i(k_z z + m\phi - \omega t)}$ is omitted in these expressions.

# Bubble Wakefield Acceleration on Soft Surface

## Positron beam-driven & self-modulation regime

Bubble wakefield

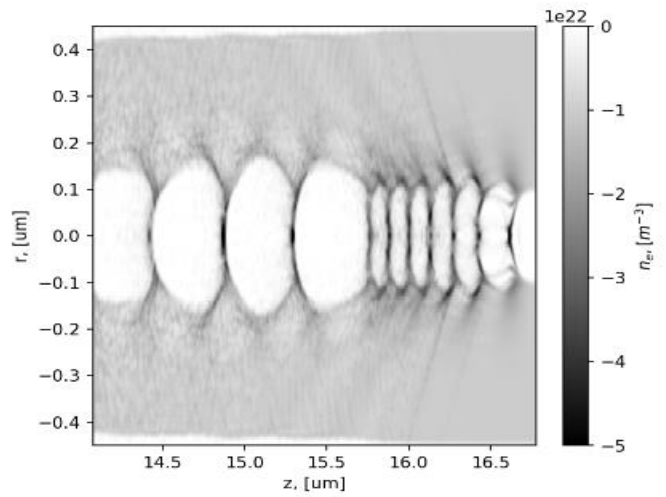


Acceleration field

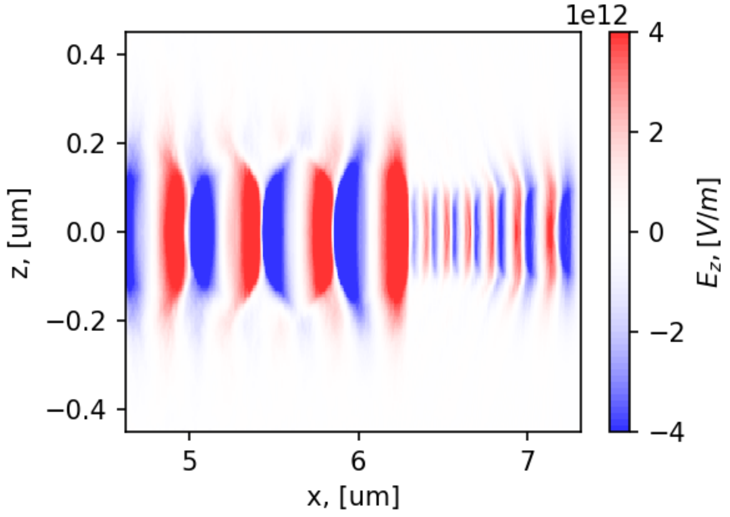


Acceleration field: 4 TV/m

Self-modulation

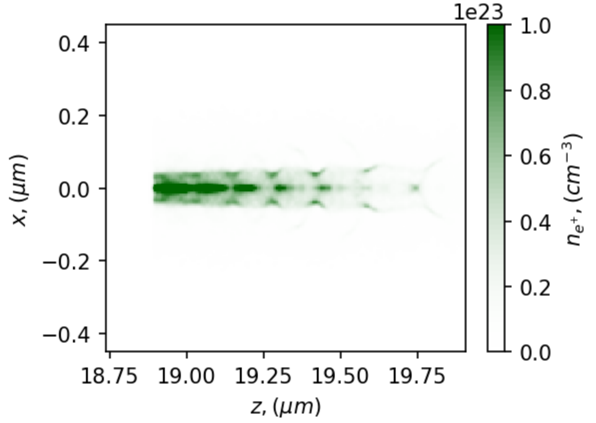


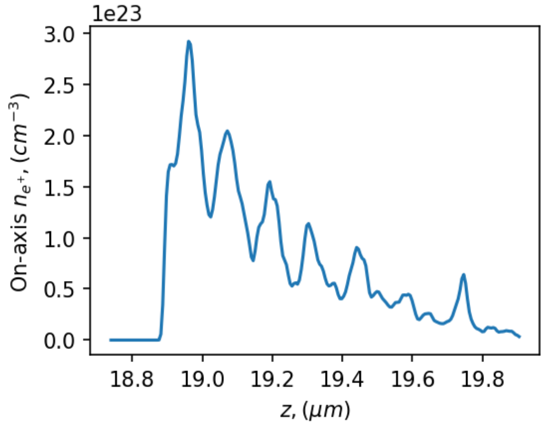

# Wave equations in General

## Curvature effects

Curvature introduces two effects:

- Dispersion shift
- High-density cut of

High-density cut-off threshold for $m = 0$ mode:

$$n_{\text{cut}} = \gamma_q \chi^2 n_c,$$

required by the dispersion condition

$$D(\omega/c^{+}) > 0$$

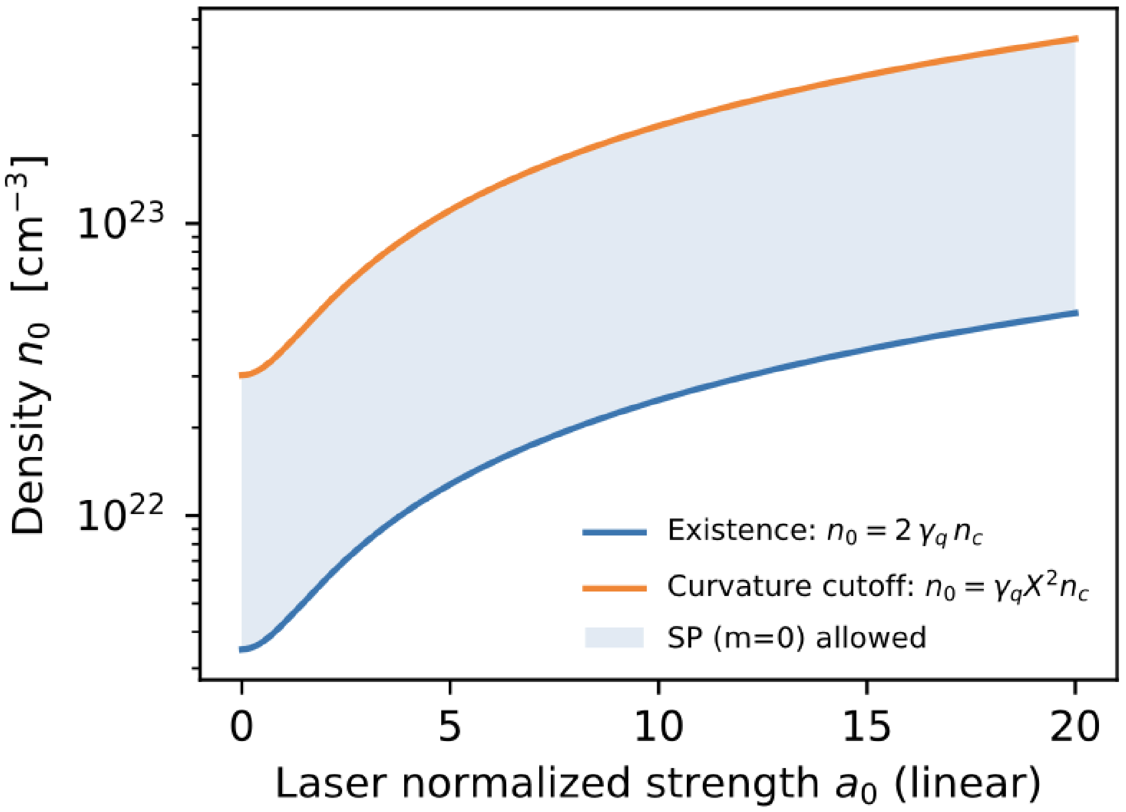

# Sharp Surface Threshold

## @3D PIC simulations

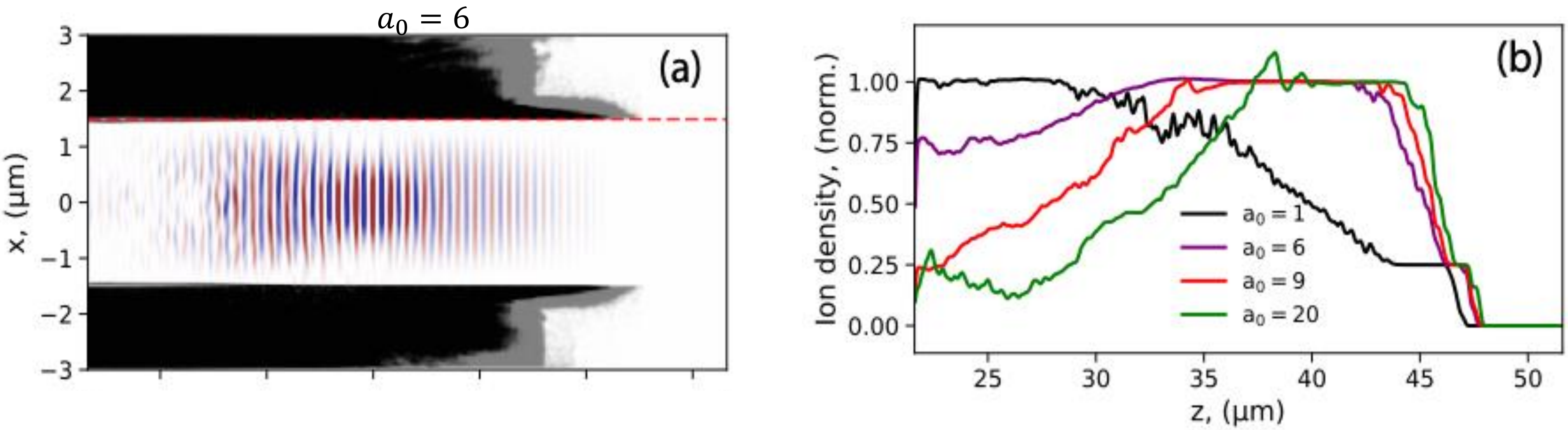

# Major Conclusions

- General theoretical frame of RSP and wakefield excitation can be obtained.
- Relativistic effects lead to the saturation of SP mode and weaker mode confinement to the interface, which enables the highly nonlinear bubble wakefield.
- Relativistic effects lead to the phase slowdown.
- Geometric effects lead to the phase shift and high-density cut-off.
- Cylindrical surface can support on-axis acceleration field, especially $m = 0$ mode, beneficial for particle acceleration.
- Soft surface can significantly modify the mode coupling.
- A new theory paper of RSP is in preparation.

# Feasibility and Alignment Challenge

| Parameters | Values | Experimental minimum |
|---|---|---|
| Laser strength, $a_0$ | 6 | $> 1$ |
| Laser RMS waist, $w_0$ | 2 $\mu$m | Several $\mu$m |
| Laser RMS duration, | $\sigma_\tau = 20$ fs | $> \lambda_p$ |
| Laser CP ellipticity, $\epsilon_L$ | 1 | $> 0.95$ |
| Laser radial offset, $\delta r$ | 0 | $< 10\%$ |
| Laser contrast ratio | $10^{-11}$ | $\leq 10^{-10}$ |
| Inner radius of microtube, $a$ | 1.5 $\mu$m | $0.5w_0 < a < 1.5w_0$ |
| Wall thickness, $w_t$ | 3 $\mu$m | $> 1$ $\mu$m |
| Carbon density, $n_{C0}$ | $2 \times 10^{21}$ cm$^{-3}$ | $0.5n_{crit} < n_{C0} < 2n_{crit}$ |

Alignment Challenge